Supporting Information

Ultralarge 3d/4f Coordination Wheels: From Carboxylate/Amino Alcohol-Supported $\{Fe_4Ln_2\}$ to $\{Fe_{18}Ln_6\}$ Rings

Olga Botezat,[†,‡] Jan van Leusen,[‡] Victor Ch. Kravtsov, [†] Paul Kögerler*[,‡] and Svetlana G. Baca*[,†]

[†]*Institute of Applied Physics, Academy of Sciences of Moldova, 2028 Chisinau, Moldova*

[‡] *Institute of Inorganic Chemistry, RWTH Aachen University, 52074 Aachen, Germany*

Corresponding Authors

* E-mail: paul.koegerler@ac.rwth-aachen.de (P.K.);

sbaca_md@yahoo.com (S.G.B.)

Tel: +49-241-80-93642 (P.K.); +373-22-738154 (S.G.B.).

Fax: +49-241-80-92642 (P.K.); +373-22-738149 (S.G.B.).

Table S1. Crystal Data and Details of Structural Determinations for 1–10

	1a	**1b**	**1c**	**1d**	**2a**
Empirical formula	$C_{58}H_{118}Dy_2Fe_4N_{16}O_{26}$	$C_{58}H_{116}Er_2Fe_4N_{16}O_{26}$	$C_{58}H_{118}Fe_4Ho_2N_{16}O_{26}$	$C_{54}H_{106}Fe_4N_{16}O_{24}Tb_2$	$C_{56}H_{110}Cl_4Dy_2Fe_4N_{16}O_{24}$
M_r / g mol^{-1}	2004.08	2013.60	2008.94	1904.78	2081.80
T / K	100(2)	100(2)	100(2)	100(2)	100(2)
Wavelength / Å	0.71073	0.71073	0.71073	0.71073	0.71073
Crystal system	Triclinic	Triclinic	Triclinic	Triclinic	Triclinic
Space group	*P*-1	*P*-1	*P*-1	*P* -1	*P*-1
Unit cell dimensions					
a / Å	12.402(3)	12.346(1)	12.3487(12)	12.4023(13)	12.265(2)
b / Å	13.871(1)	13.816(1)	13.8221(14)	13.4737(13)	14.122(2)
c / Å	14.006(1)	13.959(1)	13.9621(14)	13.6951(15)	14.379(3)
α	116.359(2)°	116.184(2)°	116.250(2)°	115.683(10)°	117.466(3)°
β	97.806(2)°	98.375(2)°	98.102(2)°	101.128(9)°	101.585(4)°
γ	101.110(2)°	101.348(2)°	101.251(2)°	99.194(8)°	96.297(4)°
V / Å^3	2050.2(6)	2020.5(4)	2025.1(3)	1945.5(4)	2105.4(5)
Z, ρ / Mg m^{-3}	1, 1.623	1, 1.655	1, 1.647	1, 1.626	1, 1.642
μ / mm^{-1}	2.569	2.834	2.709	2.598	2.625
F(000)	1022	1026	1024	968	1054
Crystal size / mm^3	0.3 × 0.28 × 0.25	0.37 × 0.28 × 0.26	0.16 × 0.11 × 0.08	0.147 x 0.09 x 0.063	0.15 × 0.09 × 0.05
θ range for data collection	2.08 – 25.00°	2.41 – 24.40°	2.06 – 25.00°	3.064 – 25.00°	1.74 – 24.67°
Index ranges	$-14 \le h \le 14$, $-16 \le k \le 16$, $-16 \le l \le 16$	$-14 \le h \le 14$, $-16 \le k <= 16$, $-16 \le l \le 16$	$-14 \le h \le 14$, $-16 \le k \le 16$, $-16 \le l \le 16$	$-14 \le h \le 14$, $-16 \le k \le 15$, $-16 \le l \le 16$	$-14 \le h \le 14$, $-16 \le k \le 16$, $-16 \le l \le 16$
Reflections collected	20885	20559	22008	21615	22355
Independent reflections	7203 [R_{int} = 0.0406]	6628 [R_{int} = 0.0278]	7123 [R_{int} = 0.0370]	6831 [R_{int} = 0.0963]	7099 [R_{int} = 0.0741]
Completeness to θ_{max}	99.7%	99.9%	99.8%	97.2%	99.4%
Data / restraints / parameters	7203 / 273 / 529	6628 / 70 / 545	7123 / 137 / 550	6831 / 47 / 472	7099 / 47 / 510

Goodness-of-fit on F^2	1.172	1.070	1.090	1.033	1.050
Final R indices [$I > 2\sigma(I)$]: R_1, wR_2	0.0578, 0.1207	0.0409, 0.0970	0.0413, 0.0949	0.0710, 0.1289	0.0429, 0.0841
R indices (all data): R_1, wR_2	0.0635, 0.1230	0.0458, 0.1014	0.0486, 0.1001	0.1256, 0.1491	0.0559, 0.0899
Largest diff. peak, hole / e Å^{-3}	3.718, –1.894	4.009, –2.124	3.776, –1.588	1.755, –1.233	1.471, –1.488
	2b	**3a**	**3b**	**4**	**4a**
Empirical formula	$C_{56}H_{110}Cl_4Er_2Fe_4N_{16}O_{24}$	$C_{50}H_{104}Cl_4Dy_2Fe_4N_{22}O_{22}$	$C_{50}H_{104}Cl_4Er_2Fe_4N_{22}O_{22}$	$C_{194}H_{409}Dy_6Fe_{18}N_{43}O_{104}$	$C_{198}H_{474}Dy_6Fe_{18}N_{42}O_{132}$
M_r / g mol^{-1}	2091.32	2055.75	2065.27	6988.92	7536.46
T / K	100(2)	100(2)	100(2)	100(2)	100(2)
Wavelength / Å	0.71073	0.71073	0.71073	0.71073	0.71073
Crystal system	Triclinic	Monoclinic	Monoclinic	Triclinic	Trigonal
Space group	*P*-1	*P*2(1)/*n*	*P*2(1)/*n*	*P*-1	*R*-3
Unit cell dimensions					
a / Å	12.343(7)	10.2958(15)	10.2724(18)	15.3106(15)	37.390(6)
b / Å	14.249(8)	18.216(3)	18.155(3)	23.090(2)	37.390(6)
c / Å	14.469(8)	22.117(3)	22.010(4)	24.293(2)	25.583(4)
α	117.314(8)°	90°	90°	78.069(3)°	90°
β	101.602(9)°	101.309(3)°	101.291(3)°	81.833(3)°	90°
γ	96.385(9)°	90°	90°	76.573(3)°	120°
V / Å^3	2153(2)	4067.4(10)	4025.3(12)	8132.8(14)	30974(11)
Z, ρ / Mg m^{-3}	1, 1.613	2, 1.679	2, 1.704	1, 1.427	3, 1.212
μ / mm^{-1}	2.781	2.717	2.974	2.212	1.752
F(000)	1058	2076	2084	3570	11628
Crystal size / mm^3	0.12 × 0.09 × 0.08	0.11 × 0.09 × 0.08	0.16 × 0.09 × 0.06	0.28 × 0.27 × 0.16	0.12 × 0.09 × 0.08
θ range for data collection	2.10 – 24.32°	2.05 – 23.26°	2.20 – 25.00°	1.486 – 24.41°	2.03 – 25.00°

Index ranges	$-14 \le h \le 14$, $-16 \le k \le 16$, $-16 \le l \le 16$	$-11 \le h \le 11$, $-20 \le k \le 20$, $-24 \le l \le 24$	$-12 \le h \le 12$, $-21 \le k \le 21$, $-26 \le l \le 26$	$-17 \le$ h ≤ 17, $-26 \le$ k ≤ 26, $-28 \le$ l ≤ 28	$-44 \le h \le 44$, $-44 \le k \le 44$, $-30 \le l \le 30$
Reflections collected	21177	36568	42222	87050	107548
Independent reflections	7001 [R_{int} = 0.1052]	5840 [R_{int} = 0.1044]	7093 [R_{int} = 0.1154]	26779 [R_{int} = 0.1050]	12120 [R_{int} = 0.1294]
Completeness to θ_{max}	99.4%	99.9%	100.0%	90.9 %	97.3%
Data / restraints / parameters	7001 / 43 / 516	5840 / 31 / 465	7093 / 42 / 476	26779 / 496 / 1752	12120 / 78 / 692
Goodness-of-fit on F^2	0.991	1.357	1.209	1.036	1.100
Final R indices [$I > 2\sigma(I)$]: R_1, wR_2	0.0548, 0.1321	0.0992, 0.2103	0.0761, 0.1627	0.0783, 0.2076	0.0623, 0.1638
R indices (all data): R_1, wR_2	0.0675, 0.1411	0.1146, 0.2161	0.1010, 0.1734	0.1309, 0.2443	0.0948, 0.1853
Largest diff. peak, hole / e Å^{-3}	3.084, –1.706	2.056, –2.248	2.401, –2.406	3.833, –2.308	2.044, –1.006
	5	**6**	**7**	**8**	**9**
Empirical formula	$C_{194}H_{413}Fe_{18}Gd_6N_{43}O_{106}$	$C_{206}H_{444}Fe_{18}N_{45}O_{110.50}Tb_6$	$C_{197}H_{427}Fe_{18}Ho_6N_{43}O_{110}$	$C_{212}H_{503}Fe_{18}N_{45}O_{134}Sm_6$	$C_{201}H_{432}Eu_6Fe_{18}N_{44}O_{109}$
M_r / g mol^{-1}	6993.45	7278.88	7153.67	7734.96	7126.94
T / K	100(2)	100(2)	100(2)	100(2)	100(2)
Wavelength / Å	0.71073	0.71073	0.71073	0.71073	0.71073
Crystal system	Triclinic	Triclinic	Triclinic	Trigonal	Triclinic
Space group	*P*-1	*P*-1	*P*-1	*R*-3	*P*-1
Unit cell dimensions					
a / Å	15.4512(18)	15.7331(6)	15.699(4)	37.438(6)	15.4184(6)
b / Å	23.102(3)	22.8661(8)	22.827(6)	37.438(6)	23.1345(9)
c / Å	24.516(3)	24.5683(9)	24.502(7)	25.744(4)	24.3653(10)
α	78.394(3)°	78.1690(10)°	78.730(5)°	90°	78.5220(10)°
β	81.559(4)°	81.1040(10)°	81.150(5)°	90°	82.0930(10)°
γ	77.193(4)°	78.1610(10)°	78.123(5)°	120°	76.8330(10)°
V / Å^3	8311.0(16)	8408.1(5)	8367(4)	31249(11)	8254.5(6)

Z, ρ / Mg m^{-3}	1, 1.397	1, 1.438	1, 1.420	3, 1.233	1, 1.434
μ / mm^{-1}	2.014	2.073	2.232	1.509	1.965
F(000)	3578	3737	3660	12006	3664
Crystal size / mm^3	0.20 × 0.10 × 0.09	0.12 × 0.10 × 0.10	0.21 × 0.20 × 0.13	0.20 × 0.16 × 0.12	0.17 × 0.13 × 0.12
θ range for data collection	1.71 – 23.26°	1.71 – 25.00°	1.50 – 25.00°	2.02 – 25.00°.	1.714 – 25.00°
Index ranges	$-17 \le h \le 17$, $-25 \le k \le 25$, $-27 \le l \le 27$	$-18 \le h \le 18$, $-27 \le k \le 27$, $-29 \le l \le 29$	$-18 \le h \le 18$, $-27 \le k \le 27$, $-29 \le l \le 29$	$-44 \le h \le 44$, $-44 \le k \le 44$, $-30 \le l \le 30$	$-18 \le h \le 18$, $-27 \le k \le 27$, $-28 \le l \le 28$
Reflections collected	77638	93450	90529	110848	89202
Independent reflections	23844 [R_{int} = 0.1559]	29594 [R_{int} = 0.0937]	29440 [R_{int} = 0.0992]	12210 [R_{int} = 0.1322]	28967 [Rint = 0.0718]
Completeness to θ_{max}	99.9 %	99.9 %	99.9 %	99.8 %	99.6 %
Data / restraints / parameters	23844 / 531 / 1766	29594 / 272 / 1929	29440 / 373 / 1850	12210 / 453 / 683	28967 / 376 / 1899
Goodness-of-fit on F^2	1.008	1.015	1.004	1.096	1.008
Final R indices [$I > 2\sigma(I)$]: R_1, wR_2	0.0834, 0.2276	0.0579, 0.1463	0.0830, 0.2231	0.0533, 0.1430	0.0598, 0.1543
R indices (all data): R_1, wR_2	0.1773, 0.2829	0.0950, 0.1710	0.1172, 0.2577	0.1016, 0.1966	0.0945, 0.1839
Largest diff. peak, hole / e Å^{-3}	1.720, –1.719	1.645, –1.236	4.050, –3.006	1.399, –1.287	1.924, –1.651
	10				
Empirical formula	$C_{207}H_{457}Fe_{18}N_{45}O_{116}Y_6$				
M_r / g mol^{-1}	6971.91				
T / K	100(2)				
Wavelength / Å	0.71073				
Crystal system	Triclinic				
Space group	P-1				
Unit cell dimensions					
a / Å	15.7078(12)				
b / Å	22.8333(17)				

c / Å	24.5202(18)				
α	78.380(2)°				
β	81.161(2)°				
γ	78.225(2)°				
V / Å^3	8374.6(11)				
Z, ρ / Mg m^{-3}	1, 1.382				
μ / mm^{-1}	1.862				
F(000)	3644				
Crystal size / mm^3	0.23 × 0.22 × 0.19				
θ range for data collection	1.365 – 25.05°				
Index ranges	$-18 \leq h \leq 18$, $-27 \leq k \leq 27$, $-29 \leq l \leq 29$				
Reflections collected	92964				
Independent reflections	29647 [R_{int} = 0.1295]				
Completeness to θ_{max}	99.9%				
Data / restraints / parameters	29651 / 71 / 1816				
Goodness-of-fit on F^2	1.008				
Final R indices [$I > 2\sigma(I)$]: R_1, wR_2	0.0613, 0.1386				
R indices (all data): R_1, wR_2	0.1283, 0.1489				
Largest diff. peak, hole / e Å^{-3}	1.293, –0.798				

Table S2. Selected Bond Distances (Å) for 1–10

1a		**1b**		**1c**		**1d**		**2a**		**2b**		**3a**		**3b**	
Dy1-O2	2.277(3)	Er1-O1	2.258(4)	Ho1-O3	2.271(4)	Tb1-O8	2.290(6)	Dy1-O2	2.283(4)	Er1-O5	2.271(5)	Dy1-O2	2.297(1)	Er1-O1	2.279(7)
Dy1-O4	2.290(5)	Er1-O5	2.269(4)	Ho1-O4	2.282(4)	Tb1-O10	2.294(6)	Dy1-O5	2.296(4)	Er1-O1	2.285(5)	Dy1-O1	2.300(1)	Er1-O2	2.280(8)
Dy1-O1	2.312(3)	Er1-O3	2.293(4)	Ho1-O1	2.297(4)	Tb1-O7	2.313(6)	Dy1-O1	2.307(4)	Er1-O4	2.312(5)	Dy1-O4	2.300(1)	Er1-O4	2.288(8)
Dy1-O6	2.326(5)	Er1-O6	2.299(4)	Ho1-O5	2.301(4)	Tb1-O11	2.337(6)	Dy1-O4	2.315(4)	Er1-O2	2.315(5)	Dy1-O5	2.311(1)	Er1-O5	2.288(7)
Dy1-O5	2.392(5)	Er1-O4	2.351(4)	Ho1-O6	2.368(4)	Tb1-O12	2.389(6)	Dy1-O3	2.393(4)	Er1-O6	2.384(5)	Dy1-O6	2.384(1)	Er1-O6	2.347(8)
Dy1-O3	2.422(3)	Er1-O2	2.380(4)	Ho1-O2	2.389(4)	Tb1-O9	2.398(6)	Dy1-O6	2.399(4)	Er1-O3	2.398(5)	Dy1-O3	2.419(1)	Er1-O3	2.365(8)
Dy1-N1	2.604(6)	Er1-N2	2.579(5)	Ho1-N2	2.586(5)	Tb1-N2	2.580(9)	Dy1-N2	2.595(5)	Er1-N1	2.604(6)	Dy1-N2	2.599(1)	Er1-N1	2.566(9)
Dy1-N2	2.611(6)	Er1-N1	2.581(5)	Ho1-N1	2.592(5)	Tb1-N1	2.608(8)	Dy1-N1	2.603(5)	Er1-N2	2.606(6)	Dy1-N1	2.599(1)	Er1-N2	2.576(8)
Fe1-O6	1.951(5)	Fe1-O6	1.947(4)	Fe1-O1	1.944(4)	Fe1-O7	1.936(7)	Fe1-O4	1.941(4)	Fe1-O4	1.957(5)	Fe1-O4	1.935(1)	Fe1-O1	1.940(8)
Fe1-O2	1.968(3)	Fe1-O1	1.961(4)	Fe1-O4	1.951(4)	Fe1-O10	1.955(6)	Fe1-O2	1.950(4)	Fe1-O1	1.982(5)	Fe1-O1	1.938(1)	Fe1-O4	1.942(1)
Fe1-O7	1.970(6)	Fe1-O7	1.967(5)	Fe1-O7	1.984(4)	Fe1-O1	1.977(6)	Fe1-O7	1.971(4)	Fe1-O9	1.987(5)	Fe1-O10$^{\#1}$	2.021(1)	Fe1-O10	2.025(8)
Fe1-O9	2.061(5)	Fe1-O9	2.058(4)	Fe1-O9	2.047(4)	Fe1-O4#1	2.023(6)	Fe1-O12$^{\#1}$	2.051(4)	Fe1-O7	2.071(5)	Fe1-N6	2.041(1)	Fe1-N6	2.042(1)
Fe1-N6$^{\#1}$	2.097(6)	Fe1-N3	2.093(5)	Fe1-N6	2.085(5)	Fe1-N3	2.076(8)	Fe1-N6	2.131(5)	Fe1-N6	2.126(6)	Fe1-N9	2.136(1)	Fe1-N3	2.122(1)
Fe1-N3$^{\#1}$	2.140(6)	Fe1-N6	2.132(5)	Fe1-N3	2.136(5)	Fe1-N6	2.112(8)	Fe1-N3	2.123(5)	Fe1-N3	2.158(6)	Fe1-N3	2.137(1)	Fe1-N9	2.131(9)
Fe2-O1	1.954(3)	Fe2-O3$^{\#1}$	1.938(4)	Fe2-O5	1.949(4)	Fe2-O11	1.947(6)	Fe2-O1	1.944(4)	Fe2-O2	1.960(5)	Fe2-O2	1.932(1)	Fe2- O2	1.923(7)
Fe2-O4	1.955(5)	Fe2-O5$^{\#1}$	1.953(4)	Fe2-O3	1.956(4)	Fe2-O5	1.961(7)	Fe2-O5	1.958(4)	Fe2-O5	1.973(5)	Fe2-O5	1.948(1)	Fe2-O5	1.939(7)
Fe2-O11	1.992(5)	Fe2-O11	1.986(4)	Fe2-O11	1.965(4)	Fe2-O8	1.970(6)	Fe2-O9	1.970(4)	Fe2-O11	1.988(5)	Fe2-O7	1.968(1)	Fe2-O7	1.967(8)
Fe2-O10	2.058(5)	Fe2-O10	2.045(4)	Fe2-O10	2.056(4)	Fe2-O3	2.061(6)	Fe2-O11	2.048(4)	Fe2-O8$^{\#1}$	2.065(5)	Fe2-O9	2.057(1)	Fe2-O9	2.049(8)
Fe2-N6	2.087(6)	Fe2-N3	2.090(5)	Fe2-N6$^{\#1}$	2.097(5)	Fe2-N3$^{\#1}$	2.079(8)	Fe2-N6$^{\#1}$	2.108(5)	Fe2-N6$^{\#1}$	2.139(6)	Fe2-N3$^{\#1}$	2.111(1)	Fe2-N3$^{\#1}$	2.103(9)
Fe2-N3	2.142(6)	Fe2-N6	2.131(5)	Fe2-N3$^{\#1}$	2.131(5)	Fe2-N6$^{\#1}$	2.100(9)	Fe2-N3$^{\#1}$	2.144(5)	Fe2-N3$^{\#1}$	2.155(6)	Fe2-N9$^{\#1}$	2.130(1)	Fe2-N9$^{\#1}$	2.139(9)
Dy1···Fe2	3.382(1)	Er1···Fe2$^{\#1}$	3.361(1)	Ho1···Fe1	3.365(1)	Tb1-Fe1	3.3780(1)	Dy1···Fe2	3.379(1)	Er1···Fe1	3.395(1)	Dy1···Fe1	3.375(3)	Er1···Fe1	3.364(1)
Dy1···Fe1	3.388(1)	Er1···Fe1	3.368(1)	Ho1···Fe2	3.372(1)	Tb1-Fe2	3.3874(1)	Dy1···Fe1	3.379(1)	Er1···Fe2	3.398(1)	Dy1···Fe2	3.393(3)	Er1···Fe2	3.375(1)
#1 -x,-y+1,-z+1		*#1 -x,-y,-z*		*#1 -x+2,-y,-z*		#1 -x+1,-y,-z		*#1 -x+2,-y,-z*		*#1 -x+2,-y,-z*		*#1 -x+1,-y,-z*		*#1 -x+2,-y,-z*	

4		**4a**		**5**		**6**		**7**		**9**		**10**	
Dy1-O31	2.310(9)	Dy1-O6	2.310(5)	Gd1-O14	2.349(11)	Tb1-O1	2.336(6)	Ho1-O14	2.320(7)	Eu1-O22	2.354(6)	Y1-O15	2.313(5)
Dy1-O33	2.312(9)	Dy1-O15$^{\#1}$	2.315(5)	Gd1-O3	2.351(11)	Tb1-O14	2.337(6)	Ho1-O15	2.331(8)	Eu1-O25	2.366(5)	Y1-O1	2.315(5)
Dy1-O3	2.323(1)	Dy1-O7$^{\#1}$	2.320(5)	Gd1-O16	2.350(11)	Tb1-O15	2.347(5)	Ho1-O1	2.338(8)	Eu1-O24	2.366(6)	Y1-O14	2.325(5)
Dy1-O16	2.342(7)	Dy1-O8	2.322(5)	Gd1-O22	2.352(11)	Tb1-O47$^{\#1}$	2.359(5)	Ho1-O47$^{\#1}$	2.339(7)	Eu1-O3	2.380(7)	Y1-O47$^{\#1}$	2.325(5)
Dy1-O2	2.346(9)	Dy1-O1	2.354(6)	Gd1-O15	2.364(11)	Tb1-O3	2.363(5)	Ho1-O16	2.347(7)	Eu1-O20	2.382(5)	Y1-O3	2.339(5)
Dy1-O13	2.352(8)	Dy1-O3	2.383(6)	Gd1-O2	2.404(11)	Tb1-O16	2.369(5)	Ho1-O3	2.354(7)	Eu1-O2	2.403(6)	Y1-O16	2.348(5)
Dy1-O32	2.381(1)	Dy1-O5	2.421(6)	Gd1-O13	2.422(11)	Tb1-O13	2.405(5)	Ho1-O13	2.372(8)	Eu1-O23	2.418(7)	Y1-O13	2.377(5)
Dy1-N7	2.681(1)	Dy1-N1	2.602(7)	Gd1-N1	2.645(14)	Tb1-N1	2.672(7)	Ho1-N1	2.652(10)	Eu1-N4	2.683(10)	Y1-N1	2.649(6)
Dy2-O7	2.304(1)	Fe1-O6	1.943(5)	Gd2-O31	2.354(11)	Tb2-O5	2.293(7)	Ho2-O5	2.274(9)	Eu2-O7	2.342(6)	Y2-O5	2.259(6)
Dy2-O37	2.309(9)	Fe1-O8	1.949(5)	Gd2-O34	2.358(10)	Tb2-O25	2.327(5)	Ho2-O25	2.314(7)	Eu2-O36	2.358(5)	Y2-O25	2.311(5)
Dy2-O39	2.323(8)	Fe1-O11	1.977(5)	Gd2-O7	2.365(13)	Tb2-O27	2.345(5)	Ho2-O27	2.318(7)	Eu2-O34	2.363(5)	Y2-O27	2.315(5)
Dy2-O20	2.339(9)	Fe1-O9	2.026(5)	Gd2-O32	2.372(14)	Tb2-O23	2.356(5)	Ho2-O23	2.336(7)	Eu2-O37	2.376(5)	Y2-O23	2.337(5)
Dy2-O22	2.342(8)	Fe1-O4	2.028(6)	Gd2-O6	2.387(12)	Tb2-O28	2.371(5)	Ho2-O28	2.363(7)	Eu2-O32	2.394(5)	Y2-O28	2.343(5)
Dy2-O6	2.364(9)	Fe1-N2	2.260(7)	Gd2-O29	2.393(11)	Tb2-O7	2.397(5)	Ho2-O7	2.385(8)	Eu2-O6	2.421(5)	Y2-O7	2.364(5)
Dy2-O38	2.419(1)	Fe2-O13	1.899(5)	Gd2-O33	2.417(13)	Tb2-O26	2.429(6)	Ho2-O26	2.407(7)	Eu2-O35	2.448(6)	Y2-O26	2.402(5)
Dy2-N9	2.652(1)	Fe2-O14	1.990(5)	Gd2-N7	2.698(16)	Tb2-N5	2.652(7)	Ho2-N5	2.624(9)	Eu2-N8	2.670(6)	Y2-N5	2.639(6)
Dy3-O44	2.321(8)	Fe2-O12	2.017(5)	Gd3-O11	2.300(13)	Tb3-O9	2.333(6)	Ho3-O37	2.303(8)	Eu3-O11	2.352(6)	Y3-O38	2.301(5)
Dy3-O11	2.321(8)	Fe2-O9	2.020(5)	Gd3-O45	2.321(11)	Tb3-O37	2.333(6)	Ho3-O39	2.311(7)	Eu3-O46	2.361(6)	Y3-O35	2.324(5)
Dy3-O45	2.329(8)	Fe2-O11	2.030(5)	Gd3-O43	2.347(10)	Tb3-O35	2.338(5)	Ho3-O35	2.330(7)	Eu3-O13	2.368(5)	Y3-O37	2.325(5)

Dy3-O28	2.333(8)	Fe2-N3	2.265(7)	Gd3-O46	2.362(9)	Tb3-O39	2.342(5)	Ho3-O9	2.331(8)	Eu3-O48	2.372(5)	Y3-O9	2.326(5)
Dy3-O26	2.346(8)	Fe3-O7	1.966(5)	Gd3-O41	2.369(10)	Tb3-O11	2.362(6)	Ho3-O11	2.343(8)	Eu3-O44	2.381(5)	Y3-O40	2.340(5)
Dy3-O10	2.355(8)	Fe3-O15	1.984(5)	Gd3-O10	2.431(11)	Tb3-O40	2.364(5)	Ho3-O40	2.358(7)	Eu3-O10	2.407(5)	Y3-O11	2.343(5)
Dy3-O43	2.381(8)	Fe3-O14	1.998(5)	Gd3-O44	2.442(11)	Tb3-O38	2.428(6)	Ho3-O38	2.392(8)	Eu3-O47	2.419(5)	Y3-O39	2.394(5)
Dy3-N11	2.654(1)	Fe3-O12	2.020(5)	Gd3-N11	2.687(14)	Tb3-N9	2.686(7)	Ho3-N9	2.663(11)	Eu3-N12	2.680(7)	Y3-N9	2.671(6)
Fe1-O33	1.918(9)	Fe3-N5	2.028(7)	Fe1-O45	1.942(11)	Fe1-O15	1.945(5)	Fe1-O15	1.933(8)	Fe1-O48	1.933(6)	Fe1-O16	1.942(5)
Fe1-O13	1.949(8)	Fe3-N4	2.308(6)	Fe1-O46	1.973(10)	Fe1-O16	1.952(5)	Fe1-O16	1.952(8)	Fe1-O13	1.986(6)	Fe1-O15	1.958(5)
Fe1-O46$^{\#1}$	1.971(8)	Dy1-Fe1	3.378(1)	Fe1-O47	1.980(11)	Fe1-O19	1.965(6)	Fe1-O19	1.968(8)	Fe1-O14	1.994(6)	Fe1-O19	1.982(5)
Fe1-O14$^{\#1}$	2.018(8)	Fe1···Fe2	3.160(2)	Fe1-O21$^{\#1}$	2.008(10)	Fe1-O17	2.020(5)	Fe1-O17	2.023(7)	Fe1-N13	2.009(10)	Fe1-O4	2.027(5)
Fe1-O1	2.040(9)	Fe2···Fe3	3.200(2)	Fe1-N19	2.046(17)	Fe1-O4	2.034(6)	Fe1-O4	2.045(8)	Fe1-O17$^{\#1}$	2.039(6)	Fe1-O17	2.028(5)
Fe1-N1	2.210(1)	Fe3···Dy1$^{\#2}$	3.524(2)	Fe1-N12	2.273(13)	Fe1-N2	2.276(7)	Fe1-N2	2.263(10)	Fe1-N1	2.300(8)	Fe1-N2	2.273(6)
Fe2-O31	1.936(8)	*#1 y+1/3,-x+y+2/3,-z+2/3*		Fe2-O20	1.877(13)	Fe2-O20	1.905(6)	Fe2-O21	1.905(9)	Fe2-O16	1.900(7)	Fe2-O20	1.887(5)
Fe2-O16	1.962(9)	*#2 x-y+1/3,x-1/3,-z+2/3*		Fe2-O47$^{\#1}$	1.996(11)	Fe2-O22	1.988(6)	Fe2-O22	1.991(8)	Fe2-O14$^{\#1}$	1.992(6)	Fe2-O22	1.987(5)
Fe2-O17	1.997(7)			Fe2-O17	2.017(11)	Fe2-O17	2.012(6)	Fe2-O17	2.013(7)	Fe2-O19	2.000(5)	Fe2-O17	2.004(5)
Fe2-N13	2.010(1)			Fe2-O19	2.021(10)	Fe2-O21	2.021(6)	Fe2-O19	2.028(8)	Fe2-O17	2.026(6)	Fe2-O21	2.024(5)
Fe2-O36	2.016(8)			Fe2-O21	2.045(10)	Fe2-O19	2.037(5)	Fe2-O20	2.030(8)	Fe2-O18	2.033(6)	Fe2-O19	2.030(5)
Fe2-N2	2.280(1)	**8**		Fe2-N3	2.277(14)	Fe2-N3	2.272(8)	Fe2-N3	2.277(10)	Fe2-N2	2.252(7)	Fe2-N3	2.243(7)
Fe3-O35	1.897(8)			Fe3-O14	1.921(11)	Fe3-O25	1.953(5)	Fe3-O25	1.955(7)	Fe3-O22	1.931(6)	Fe3-O25	1.953(5)
Fe3-O19	1.998(8)	Sm1-O15$^{\#1}$	2.372(5)	Fe3-O19	1.946(11)	Fe3-O23	1.985(6)	Fe3-O23	1.981(8)	Fe3-O18	1.963(6)	Fe3-O22	1.983(5)
Fe3-O17	1.998(7)	Sm1-O8	2.380(5)	Fe3-O16	1.951(11)	Fe3-O22	1.989(6)	Fe3-O22	1.997(8)	Fe3-O20	1.968(5)	Fe3-O23	1.991(5)
Fe3-O36	2.022(7)	Sm1-O7	2.381(5)	Fe3-O17	2.015(10)	Fe3-O21	2.013(5)	Fe3-O20	2.014(7)	Fe3-O19	2.032(6)	Fe3-N13	1.994(8)
Fe3-O34	2.039(8)	Sm1-O6	2.392(5)	Fe3-O1	2.036(11)	Fe3-N13	2.037(8)	Fe3-N13	2.043(9)	Fe3-O1	2.043(6)	Fe3-O21	2.013(5)
Fe3-N8	2.263(1)	Sm1-O3	2.403(5)	Fe3-N2	2.281(14)	Fe3-N4	2.283(7)	Fe3-N4	2.281(9)	Fe3-N3	2.225(7)	Fe3-N4	2.275(6)
Fe4-O39	1.942(8)	Sm1-O1	2.454(6)	Fe4-O15	1.939(12)	Fe4-O27	1.948(5)	Fe4-O27	1.955(7)	Fe4-O24	1.943(6)	Fe4-O27	1.944(5)
Fe4-O20	1.958(9)	Sm1-O5	2.469(6)	Fe4-O22	1.980(10)	Fe4-O28	1.958(5)	Fe4-O28	1.956(7)	Fe4-O25	1.979(6)	Fe4-O28	1.949(5)
Fe4-O34	1.968(8)	Sm1-N1	2.646(6)	Fe4-N13	1.986(17)	Fe4-O31	1.985(6)	Fe4-O31	1.987(8)	Fe4-O26	1.989(5)	Fe4-O31	1.987(5)
Fe4-O19	2.025(8)	Fe1-O7	1.943(5)	Fe4-O23	2.021(12)	Fe4-O8	2.034(5)	Fe4-O29	2.034(7)	Fe4-O29	2.011(6)	Fe4-O29	2.037(5)
Fe4-O5	2.035(8)	Fe1-O8	1.956(5)	Fe4-O25	2.037(11)	Fe4-O29	2.038(5)	Fe4-O8	2.036(7)	Fe4-N16	2.030(8)	Fe4-O8	2.041(5)
Fe4-N3	2.255(1)	Fe1-O11	1.992(5)	Fe4-N4	2.327(15)	Fe4-N6	2.280(6)	Fe4-N6	2.265(10)	Fe4-N5	2.2697	Fe4-N6	2.276(6)
Fe5-O37	1.934(8)	Fe1-O9	2.034(5)	Fe5-O26	1.916(13)	Fe5-O32	1.898(6)	Fe5-O32	1.909(8)	Fe5-O28	1.901(5)	Fe5-O33	1.907(5)
Fe5-O22	1.978(8)	Fe1-O2	2.035(5)	Fe5-O28	1.986(10)	Fe5-O34	2.002(5)	Fe5-O34	2.003(7)	Fe5-O26	1.995(5)	Fe5-O34	1.997(5)
Fe5-O23	1.985(8)	Fe1-N2	2.287(6)	Fe5-O23	1.995(12)	Fe5-O29	2.005(5)	Fe5-O29	2.012(8)	Fe5-O31	2.003(5)	Fe5-O29	2.002(5)
Fe5-N16	2.002(1)	Fe2-O13	1.910(5)	Fe5-O27	2.027(11)	Fe5-O33	2.037(5)	Fe5-O31	2.032(7)	Fe5-O29	2.019(5)	Fe5-O32	2.035(5)
Fe5-O41	2.013(8)	Fe2-O14	1.992(5)	Fe5-O25	2.044(11)	Fe5-O31	2.043(6)	Fe5-O33	2.039(8)	Fe5-O30	2.035(5)	Fe5-O31	2.041(5)
Fe5-N4	2.274(9)	Fe2-O9	2.028(5)	Fe5-N5	2.254(13)	Fe5-N7	2.274(7)	Fe5-N7	2.268(9)	Fe5-N6	2.260(7)	Fe5-N7	2.262(6)
Fe6-O42	1.884(9)	Fe2-O12	2.031(5)	Fe6-O31	1.876(12)	Fe6-O37	1.935(5)	Fe6-O37	1.947(8)	Fe6-O34	1.942(5)	Fe6-O37	1.936(5)
Fe6-O25	1.986(8)	Fe2-O11	2.045(5)	Fe6-O27	1.954(10)	Fe6-O35	1.979(6)	Fe6-O35	1.975(8)	Fe6-O32	1.956(5)	Fe6-O35	1.978(5)
Fe6-O23	1.994(8)	Fe2-N3	2.273(6)	Fe6-O29	2.002(10)	Fe6-O34	1.997(5)	Fe6-O34	1.998(7)	Fe6-O30	1.981(5)	Fe6-O34	1.986(5)
Fe6-O41	2.026(9)	Fe3-O6$^{\#2}$	1.970(5)	Fe6-O5	2.038(12)	Fe6-O33	2.016(5)	Fe6-O33	2.015(8)	Fe6-O31	2.029(5)	Fe6-O32	2.017(5)
Fe6-O40	2.040(8)	Fe3-O15	1.992(5)	Fe6-O28	2.051(11)	Fe6-N16	2.058(8)	Fe6-N16	2.050(13)	Fe6-O5	2.035(6)	Fe6-N16	2.062(8)
Fe6-N10	2.258(1)	Fe3-O14	1.999(5)	Fe6-N6	2.225(16)	Fe6-N8	2.269(7)	Fe6-N8	2.276(9)	Fe6-N7	2.261(7)	Fe6-N8	2.273(6)
Fe7-O44	1.939(8)	Fe3-O12	2.031(5)	Fe7-O32	1.923(11)	Fe7-O39	1.945(6)	Fe7-O39	1.941(8)	Fe7-O36	1.939(5)	Fe7-O38	1.929(5)
Fe7-O26	1.949(8)	Fe3-N5	2.035(7)	Fe7-O34	1.976(11)	Fe7-O43	1.955(5)	Fe7-O43	1.957(8)	Fe7-O38	1.984(6)	Fe7-O40	1.948(5)
Fe7-O40	1.954(9)	Fe3-N4	2.296(6)	Fe7-O35	2.011(9)	Fe7-O40	1.962(5)	Fe7-O40	1.957(8)	Fe7-O37	1.986(5)	Fe7-O43	1.957(5)
Fe7-O25	2.019(8)	Sm1···Fe1	3.431(1)	Fe7-O37	2.013(11)	Fe7-O41	2.039(5)	Fe7-O41	2.024(7)	Fe7-N19	2.016(9)	Fe7-O41	2.033(5)
Fe7-O9	2.036(8)	Fe1···Fe2	3.173(2)	Fe7-N16	2.04(2)	Fe7-O12	2.060(5)	Fe7-O12	2.045(8)	Fe7-O40	2.016(5)	Fe7-O12	2.046(5)
Fe7-N5	2.285(1)	Fe2···Fe3	3.204(2)	Fe7-N8	2.284(15)	Fe7-N10	2.229(7)	Fe7-N10	2.240(10)	Fe7-N9	2.266(7)	Fe7-N10	2.201(7)
Fe8-O45	1.923(9)	Fe3···Sm1	3.574(1)	Fe8-O39	1.898(11)	Fe8-O45	1.915(6)	Fe8-O44	1.914(8)	Fe8-O41	1.902(7)	Fe8-O45	1.904(5)
Fe8-O28	1.981(8)	*#1 y-1/3,-x+y+1/3,-*		Fe8-O35	1.983(10)	Fe8-O46	1.987(6)	Fe8-O46	1.979(8)	Fe8-O43	1.992(6)	Fe8-O46	1.987(5)
Fe8-N19	1.992(1)	*z+1/3*		Fe8-O40	1.993(11)	Fe8-O41	1.994(5)	Fe8-O41	1.999(7)	Fe8-O38	2.001(6)	Fe8-O41	1.993(5)

Fe8-O29	1.994(1)	*#2 x-y+2/3,x+1/3,-z+1/3*	Fe8-O37	2.016(10)	Fe8-O44	2.033(6)	Fe8-O43	2.043(8)	Fe8-O40	2.020(6)	Fe8-O44	2.031(5)
Fe8-O48	2.030(8)		Fe8-O38	2.039(10)	Fe8-O43	2.035(5)	Fe8-O45	2.045(8)	Fe8-O42	2.027(6)	Fe8-O43	2.048(5)
Fe8-N6	2.298(1)		Fe8-N9	2.289(14)	Fe8-N11	2.261(6)	Fe8-N11	2.256(10)	Fe8-N10	2.270(8)	Fe8-N11	2.258(6)
Fe9-O47	1.889(1)		Fe9-O43	1.956(11)	Fe9-O14$^{\#1}$	1.953(6)	Fe9-O14$^{\#1}$	1.940(8)	Fe9-O46	1.947(6)	Fe9-O14$^{\#1}$	1.936(5)
Fe9-O29	1.979(9)		Fe9-O38	1.971(10)	Fe9-O47	1.981(5)	Fe9-O47	1.972(8)	Fe9-O44	1.953(5)	Fe9-O46	1.983(5)
Fe9-O14	1.989(8)		Fe9-O41	1.974(10)	Fe9-O46	2.004(6)	Fe9-O46	2.005(8)	Fe9-O42	1.965(6)	Fe9-O47	1.990(5)
Fe9-O48	2.025(9)		Fe9-O9	2.021(11)	Fe9-O44	2.031(5)	Fe9-O45	2.017(8)	Fe9-O43	2.023(6)	Fe9-N19	2.010(7)
Fe9-O46	2.029(9)		Fe9-O40	2.040(11)	Fe9-N19	2.045(8)	Fe9-N19	2.064(12)	Fe9-O9	2.030(5)	Fe9-O44	2.040(5)
Fe9-N12	2.251(1)		Fe9-N10	2.273(13)	Fe9-N12	2.299(7)	Fe9-N12	2.304(11)	Fe9-N11	2.269(7)	Fe9-N12	2.300(6)
Fe1···Dy1	3.359(2)		Gd1…Fe3	3.381(2)	Tb1···Fe1	3.369(1)	Ho1···Fe1	3.357(2)	Eu1···Fe3	3.391(1)	Y1···Fe1	3.354(1)
Dy1···Fe2	3.464(2)		Gd1…Fe4	3.516(3)	Fe1···Fe2	3.174(2)	Fe1···Fe2	3.177(2)	Fe3···Fe2	3.171(2)	Fe1···Fe2	3.179(2)
Fe2···Fe3	3.205(3)		Fe4…Fe5	3.222(4)	Fe2···Fe3	3.199(2)	Fe2···Fe3	3.206(2)	Eu1···Fe4	3.501(1)	Fe2···Fe3	3.205(2)
Fe3···Fe4	3.165(3)		Fe5…Fe6	3.162(3)	Fe3···Tb2	3.511(1)	Fe3···Ho2	3.503(2)	Eu2···Fe6	3.412(1)	Y2···Fe3	3.498(1)
Fe4···Dy2	3.369(2)		Gd2…Fe6	3.389(3)	Tb2···Fe4	3.397(1)	Ho2···Fe4	3.381(2)	Eu2···Fe7	3.534(1)	Y2···Fe4	3.377(2)
Dy2···Fe5	3.490(2)		Gd2…Fe7	3.494(3)	Fe4···Fe5	3.186(2)	Fe4···Fe5	3.180(3)	Fe4···Fe5	3.201(2)	Fe4···Fe5	3.180(2)
Fe5···Fe6	3.197(2)		Fe7…Fe8	3.205(4)	Fe5···Fe6	3.209(2)	Fe5···Fe6	3.205(3)	Fe5···Fe6	3.176(2)	Fe5···Fe6	3.209(2)
Fe6···Fe7	3.168(2)		Fe8…Fe9	3.184(4)	Fe6···Tb3	3.483(1)	Fe6···Ho3	3.470(2)	Eu3···Fe9	3.387(1)	Y3···Fe6	3.469(2)
Fe7···Dy3	3.366(2)		Gd3…Fe9	3.412(2)	Tb3···Fe7	3.375(1)	Ho3···Fe7	3.361(2)	Eu3···Fe1	3.520(1)	Y3···Fe7	3.357(1)
Dy3···Fe8	3.488(2)		Gd3…Fe1	3.529(2)	Fe7···Fe8	3.164(2)	Fe7···Fe8	3.168(2)	Fe7···Fe8	3.198(2)	Fe7···Fe8	3.164(1)
Fe8···Fe9	3.211(2)		Fe1…Fe2	3.201(3)	Fe8···Fe9	3.216(2)	Fe8···Fe9	3.215(2)	Fe8···Fe9	3.178(2)	Fe8···Fe9	3.218(2)
Fe9···Fe1$^{\#1}$	3.164(2)		Fe2…Fe3	3.178(3)	Fe9···Tb1$^{\#1}$	3.506(1)	Fe9···Ho1$^{\#1}$	3.485(2)	Fe1···Fe2$^{\#1}$	3.212(2)	Y1···Fe9$^{\#1}$	3.488(1)
#1 -x+1,-y+2,-z			*#1 -x+1,-y+1,-z*		*#1 -x+2,-y+1,-z+1*		*#1 -x+1,-y,-z+1*		*#1 -x,-y+1,-z*		*#1 -x+1,-y+1,-z*	

Discussion of hydrogen bonding in compounds 1–3

In **1**–**3**, the protonated oxygen atoms of $Htea^{2-}$ ligands participate in short intramolecular O–H···O hydrogen bonds with the uncoordinated oxygen carboxylate atom (2.558(6)–2.605(7) Å) (Figs. S9, S11, S14). Additionally, the crystal solvent (EtOH) molecules form several intermolecular O–H···O and C–H···O contacts with $\{Fe_4Ln_2\}$ wheels in **1a**/**b**/**c**: with the uncoordinated O atom of pivalic acid (O–H···O: 2.675(12)–2.773(8) Å), and with $Htea^{2-}$ protons (H···O: 2.517 Å) on an adjacent $\{Fe_4Ln_2\}$ wheel, assembling hydrogen-bonded chains (Fig. S10). In **2a**/**b**, the CH_2Cl_2 solvent molecules play an important role in the organization of the hydrogen-bonded network: each solvent molecule connects three neighboring $\{Fe_4Ln_2\}$ wheels, through C–H···Cl hydrogen bonding interactions (H···Cl, 2.701–2.931 Å) between Cl atoms of dichloromethane and polyalcohol ligand protons constructing hydrogen-bonded chains as shown in Fig. S12, and through C–H···O contacts between a CH proton of methylene chloride and an uncoordinated O carboxylate atom, further bridging the chains into 2D layers (Fig. S13). The 3D hydrogen-bonded networks in **2a**/**b** are finally organized through C–H···N interactions (H···N: 2.655 Å) between CH protons of $Htea^{2-}$ and the terminal N atom of the azide groups. In **3a**/**b**, both solvent molecules, EtOH and CH_2Cl_2, participate in hydrogen bonds and induce the formation of a 3D supramolecular architecture. EtOH molecules here are involved in the formation of intermolecular O–H···N hydrogen bonds with monodentate N atoms of the azide ligands (O···N: 2.69(2) Å in **3a**; 2.731(14) Å in **3b**) and O–H···O hydrogen bonding interactions with O atom from $Htea^{2-}$ (O···O: 2.664(2) in **3a**; 2.632(12) Å in **3b**), as shown in Figure S14. Further, solvate CH_2Cl_2 molecules through C–H···O (H···O, 2.368–2.381 Å) and C–H···N (H···N, 2.704–2.741 Å) contacts between their hydrogen atoms and an uncoordinated O carboxylate atom and N atom of azide bring the adjacent wheels together and arrange the coordination wheels in **3a**/**b** into 2D hydrogen-bonded layers (Fig. S15). Finally, the terminal N atoms of the remaining azides are all involved in C–H···N contacts (H···N, 2.517–2.680 Å) with triethanolamine CH protons on the adjacent wheels and interlink the neighboring layers into a 3D network.

Table S3. Hydrogen Bonds in 1-3 [Å and °]

D–H···A	d(D–H)	d(H···A)	d(D···A)	<(DHA)
1a				
O3–H3C···O8	0.86	1.74	2.599(7)	178.1
O5–H5C···O12	0.86	1.72	2.575(8)	171.0
O13–H13D···O12$^{\#2}$	0.80	1.90	2.675(12)	164.7
#2 x, y, z+1				
1b				
O2–H2···O8	0.95	2.04	2.572(7)	113.7
O4–H4···O12$^{\#1}$	0.96	1.61	2.570(7)	174.7
O13–H13···O12$^{\#2}$	0.84	1.99	2.767(9)	154.2
#1 –x, –y, –z	*#2–x+1, –y, –z*			

1c				
O2–H2···O12	0.90	1.70	2.581(6)	166.5
O6–H6···O8	0.88	1.70	2.573(6)	169.9
O13–H13···O8	0.80	2.00	2.773(8)	163.1
1d				
O(9)-H(9)...O(6)	0.90	1.71	2.575(9)	160.9
O(12)-H(12)...O(2)	0.90	1.70	2.593(9)	170.7
2a				
O3–H3D···O8	0.86	1.72	2.558(6)	164.4
O6–H6D···O10	0.86	1.75	2.583(5)	162.7
2b				
O6–H6···O12	0.99	1.64	2.584(7)	158.3
O3–H3···O10	0.86	1.77	2.605(7)	162.6
3a				
O6–H6···O8	0.961	1.984	2.573(2)	117.5
O11–H11···N6	0.82	1.879	2.69(2)	172.1
3b				
O11–H11C···N6$^{\#2}$	0.96	1.77	2.731(14)	173.4
O6–H6C···O8	0.98	1.64	2.579(12)	159.1
O3–H3···O11$^{\#3}$	0.85	1.78	2.632(12)	179.9
#2 x, y+1, z #3 x, y–1, z				

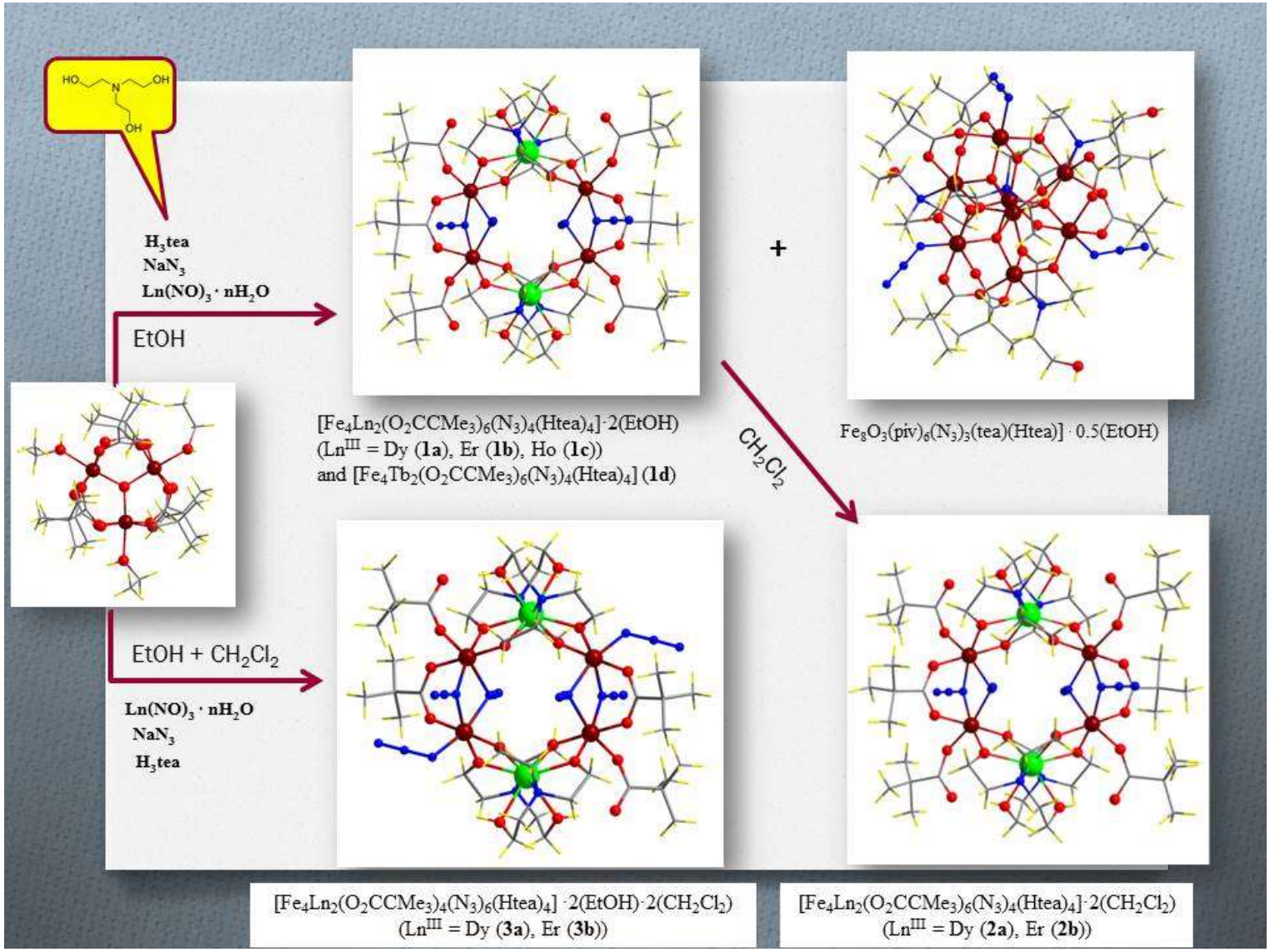

Scheme S1. Overview of synthesis routes for {Fe_4Ln_2}-type wheels (compounds **1**–**3**).

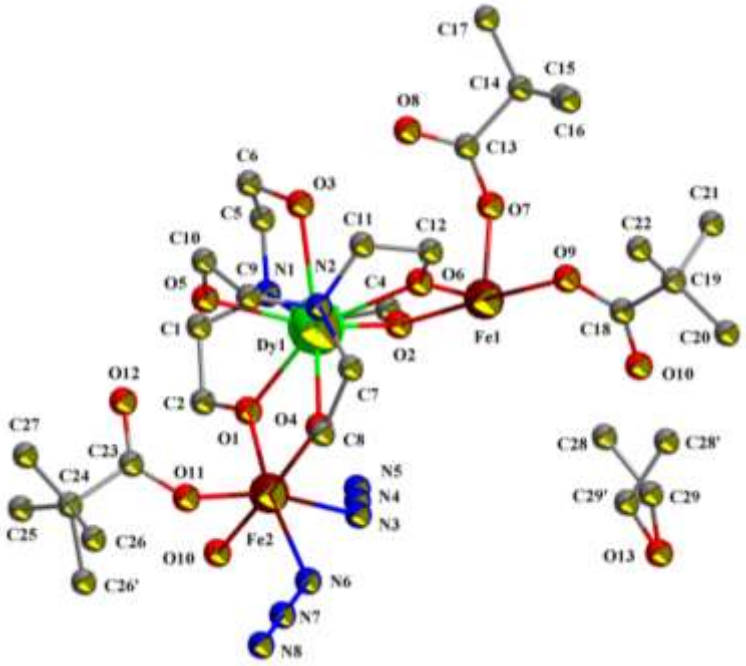

Figure S1. Asymmetric unit in the solid-state structure of $[Fe_4Dy_2(O_2CCMe_3)_6(N_3)_4(Htea)_4]\cdot 2(EtOH)$ (**1a**) with atom numbering scheme. Hydrogen atoms are omitted for clarity.

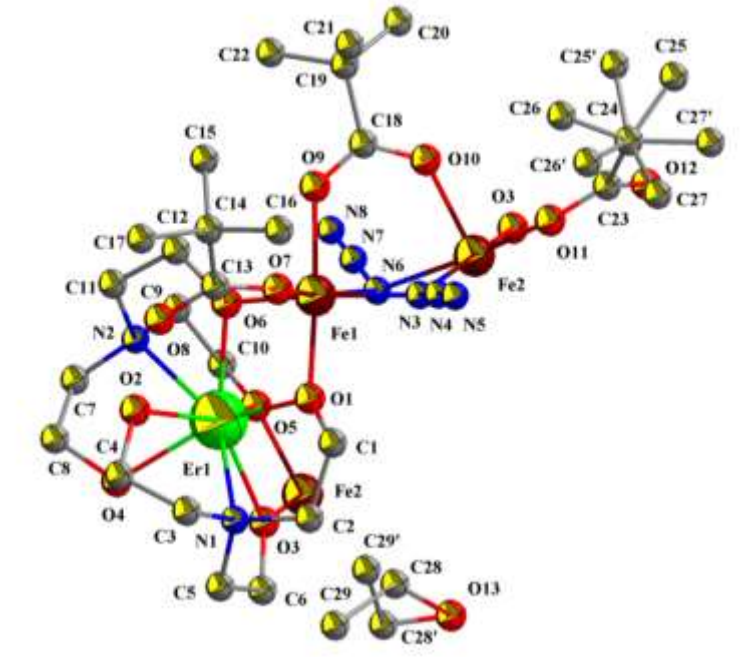

Figure S2. Asymmetric unit in the solid-state structure of $[Fe_4Er_2(O_2CCMe_3)_6(N_3)_4(Htea)_4]\cdot 2(EtOH)$ (**1b**) with atom numbering scheme. Hydrogen atoms are omitted for clarity.

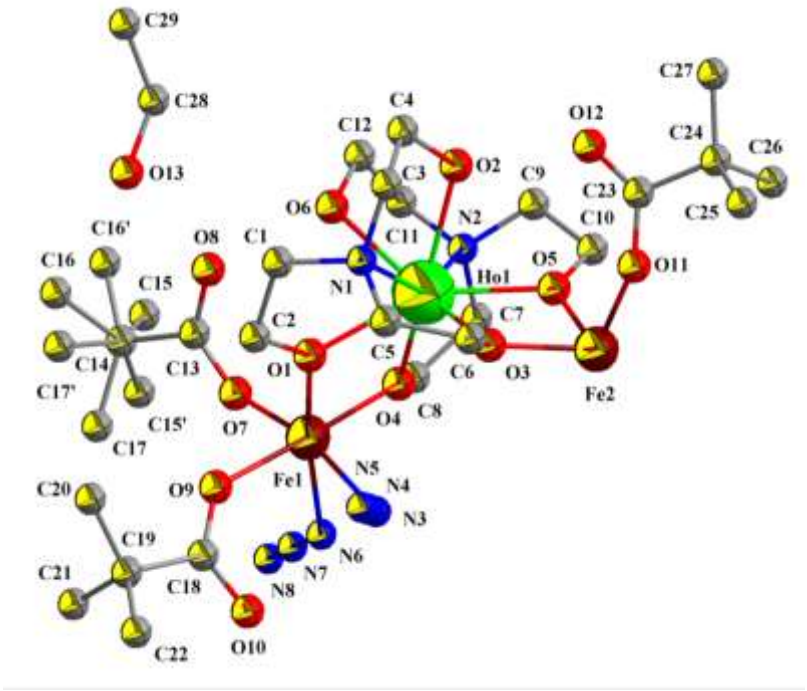

Figure S3. Asymmetric unit in the solid-state structure of $[Fe_4Ho_2(O_2CCMe_3)_6(N_3)_4(Htea)_4]\cdot 2(EtOH)$ (**1c**) with atom numbering scheme. Hydrogen atoms are omitted for clarity.

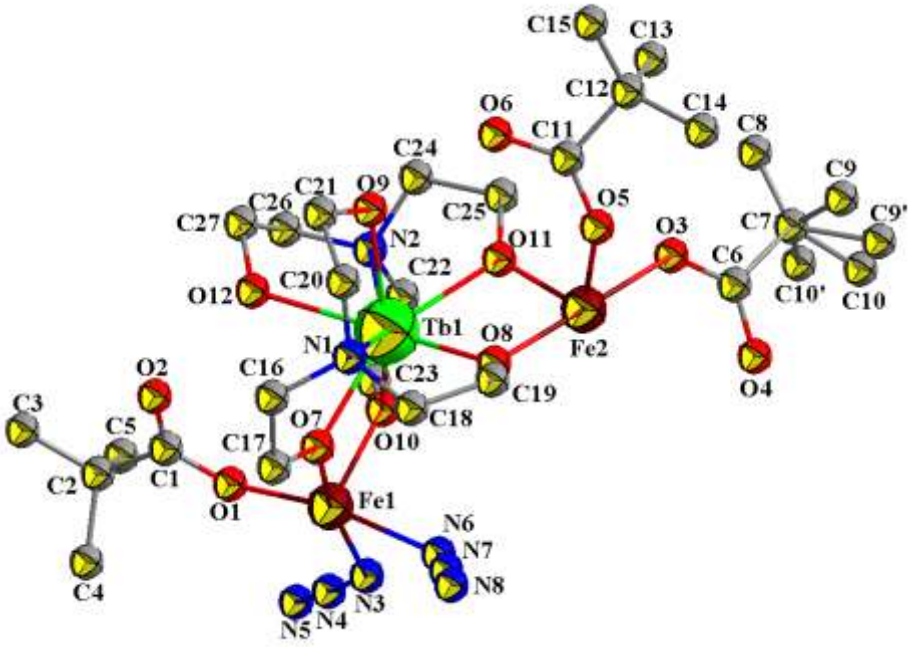

Figure S4. Asymmetric unit in the solid-state structure of $[Fe_4Tb_2(O_2CCMe_3)_6(N_3)_4(Htea)_4]$ (**1d**) with atom numbering scheme. Hydrogen atoms are omitted for clarity.

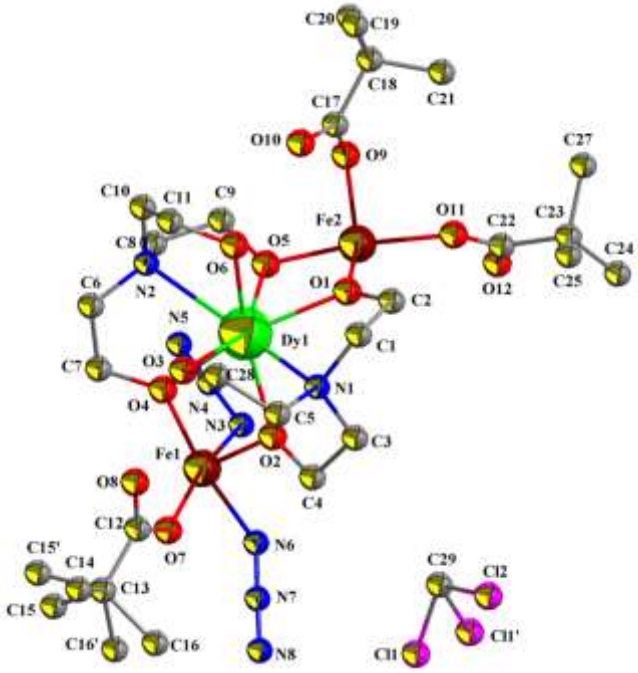

Figure S5. Asymmetric unit in the solid-state structure of $[Fe_4Dy_2(O_2CCMe_3)_6(N_3)_4(Htea)_4]\cdot 2(CH_2Cl_2)$ (**2a**) with atom numbering scheme. Hydrogen atoms are omitted for clarity.

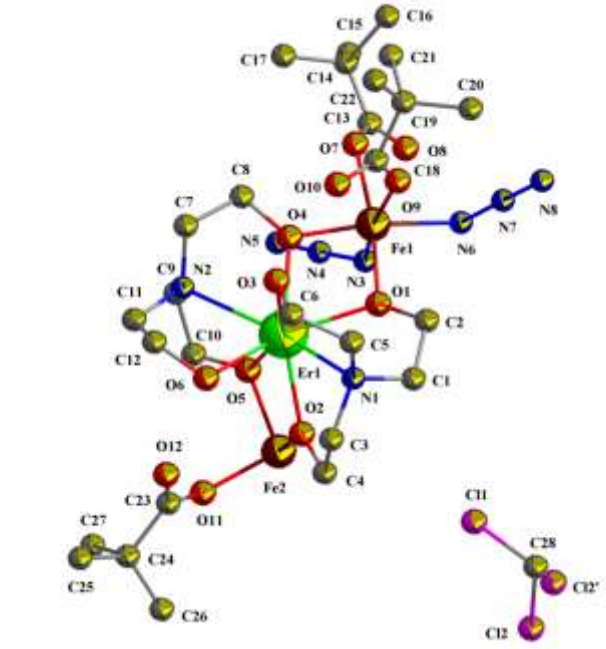

Figure S6. Asymmetric unit in the solid-state structure of $[Fe_4Er_2(O_2CCMe_3)_6(N_3)_4(Htea)_4]\cdot 2(CH_2Cl_2)$ (**2b**) with atom numbering scheme. Hydrogen atoms are omitted for clarity.

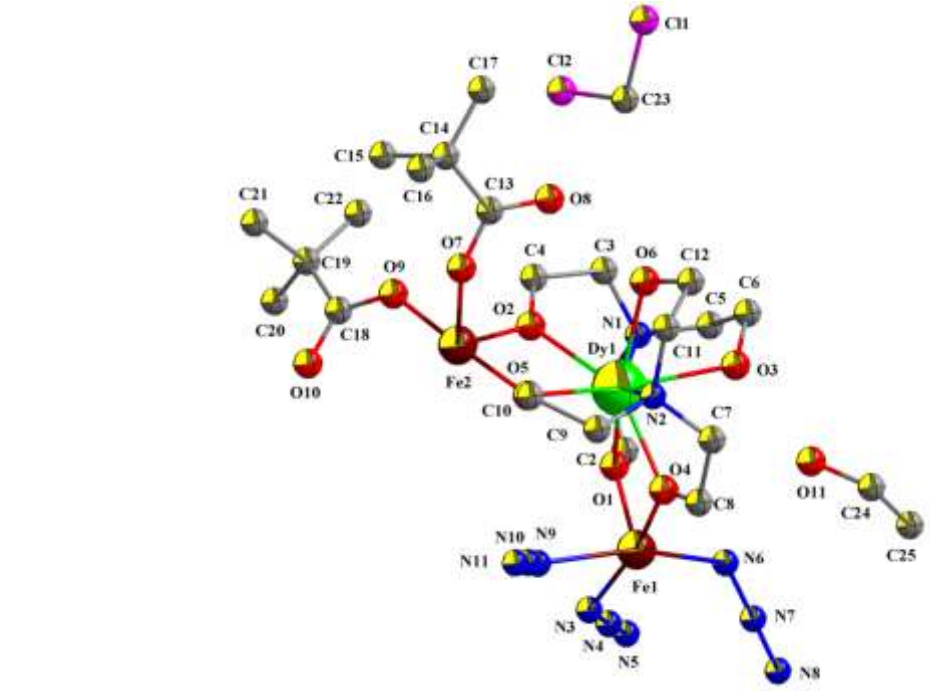

Figure S7. Asymmetric unit in the solid-state structure of $[Fe_4Dy_2(O_2CCMe_3)_4(N_3)_6(Htea)_4]\cdot 2(EtOH)\cdot 2(CH_2Cl_2)$ (**3a**) with atom numbering scheme. Hydrogen atoms are omitted for clarity.

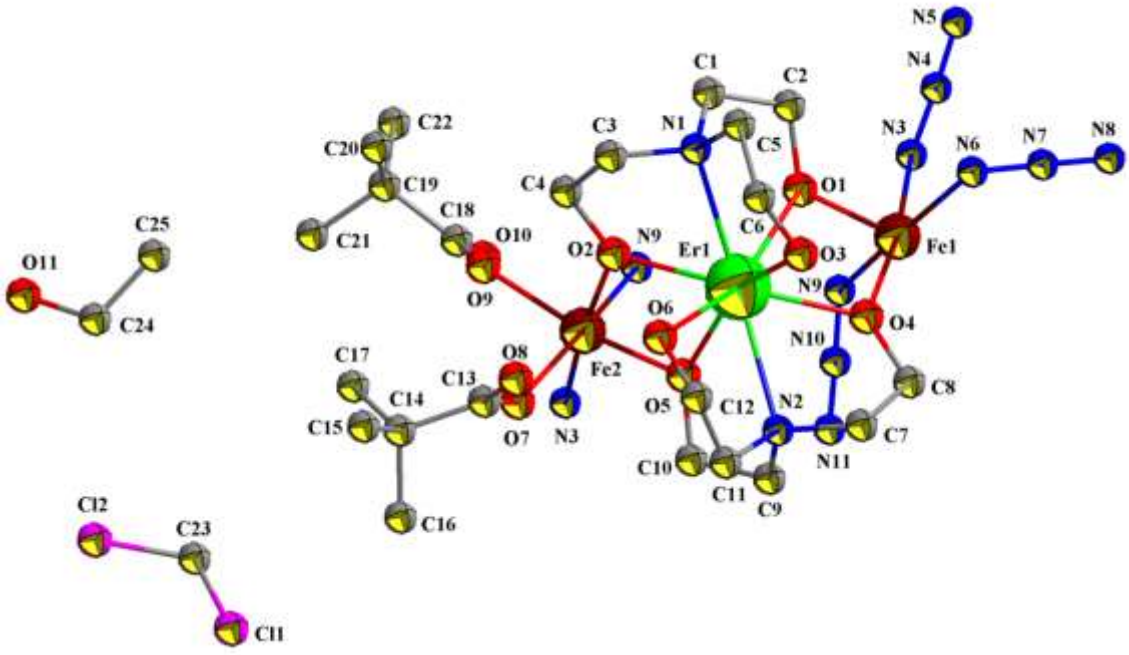

Figure S8. Asymmetric unit in the solid-state structure of $[Fe_4Er_2(O_2CCMe_3)_4(N_3)_6(Htea)_4]\cdot 2(EtOH)\cdot 2(CH_2Cl_2)$ (**3b**) with atom numbering scheme. Hydrogen atoms are omitted for clarity.

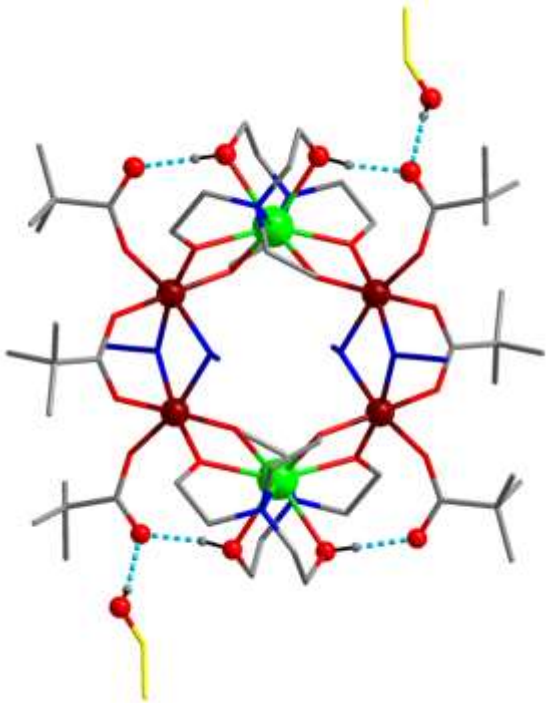

Figure S9. Intramolecular O–H···O and intermolecular O–H···O and C–H…O hydrogen bonds (dashed blue lines) formed in compounds **1a**, **1b** and **1c**. All other hydrogen atoms (except those that participate in the formation of hydrogen bonds) are omitted for clarity. Color scheme: Ln, green; Fe, brown spheres or polyhedra; O, red; N, blue; C, gray sticks. Oxygen atoms that form hydrogen bonds are shown as red spheres. Solvent ethanol molecules are highlighted in yellow.

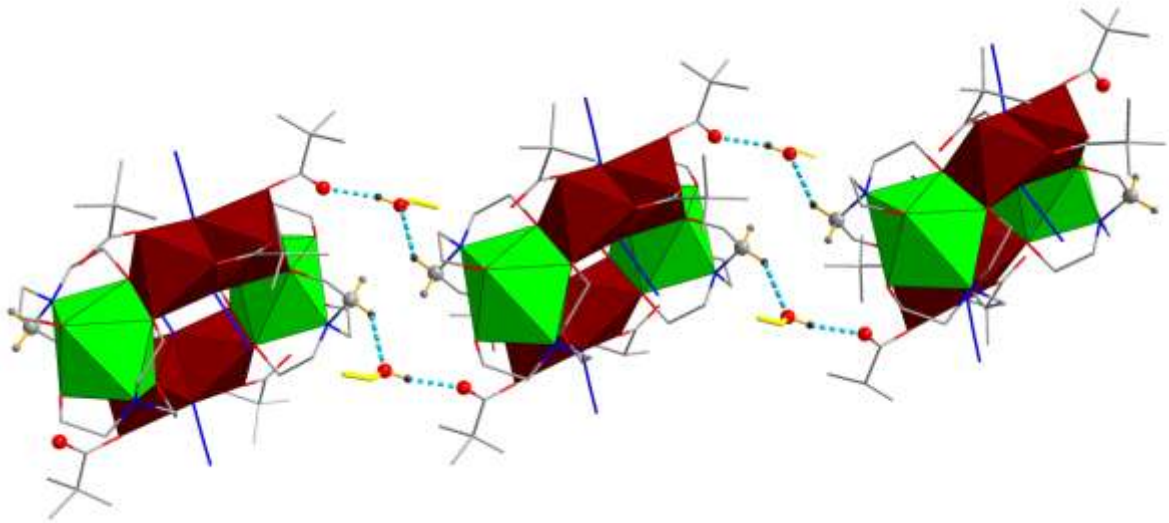

Figure S10. A view of hydrogen-bonded chain formed in compounds **1a**, **1b** and **1c**. Hydrogen bonds are shown as dashed blue lines. All other hydrogen atoms (except those that participate in the formation of hydrogen bonds) are omitted for clarity. Color scheme: Ln, green; Fe, brown polyhedra; O, red; N, blue; C, gray sticks. Oxygen atoms that form hydrogen bonds are shown as red spheres. Solvent ethanol molecules are highlighted in yellow.

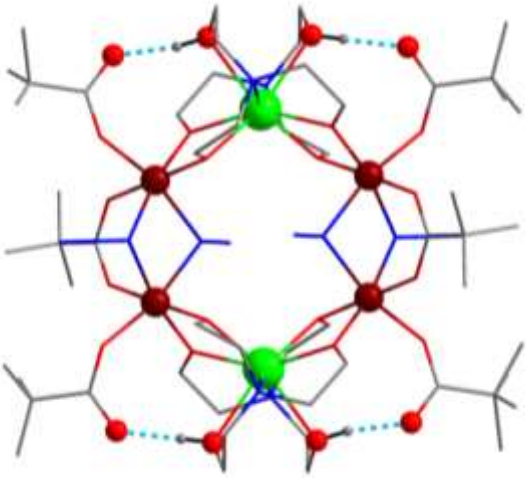

Figure S11. Intramolecular O–H···O hydrogen bonds (dashed blue lines) formed in compounds **2a** and **2b** between O atoms of triethanolamine and carboxylate ligands. All other hydrogen atoms (except those that participate in the formation of hydrogen bonds) are omitted for clarity. Color scheme: Ln, green; Fe, brown spheres; O, red; N, blue; C, gray sticks; Cl, pink spheres. Oxygen atoms that form hydrogen bonds are shown as red spheres.

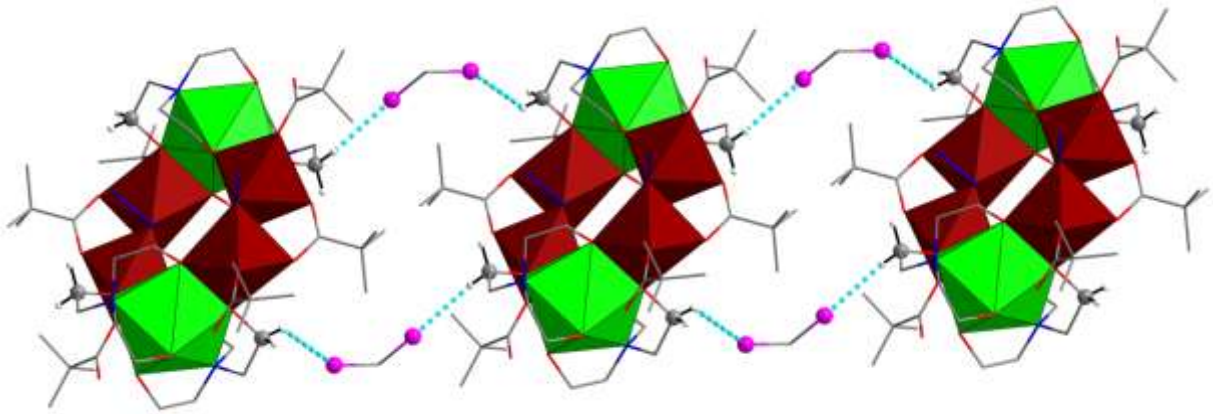

Figure S12. A fragment of the hydrogen-bonded chain formed through C–H…Cl interactions (H···Cl, 2.701 – 2.931 Å) between chlorines in CH_2Cl_2 and hydrogen atom in CH_2 group of $Htea^{2-}$ ligands in structure **2a**/**b**. Hydrogen bonds are shown as dashed blue lines. All other hydrogen atoms (except those that participate in the formation of hydrogen bonds) are omitted for clarity. Color scheme: Ln, green; Fe, brown polyhedra; O, red; N, blue; C, gray sticks; Cl, pink spheres.

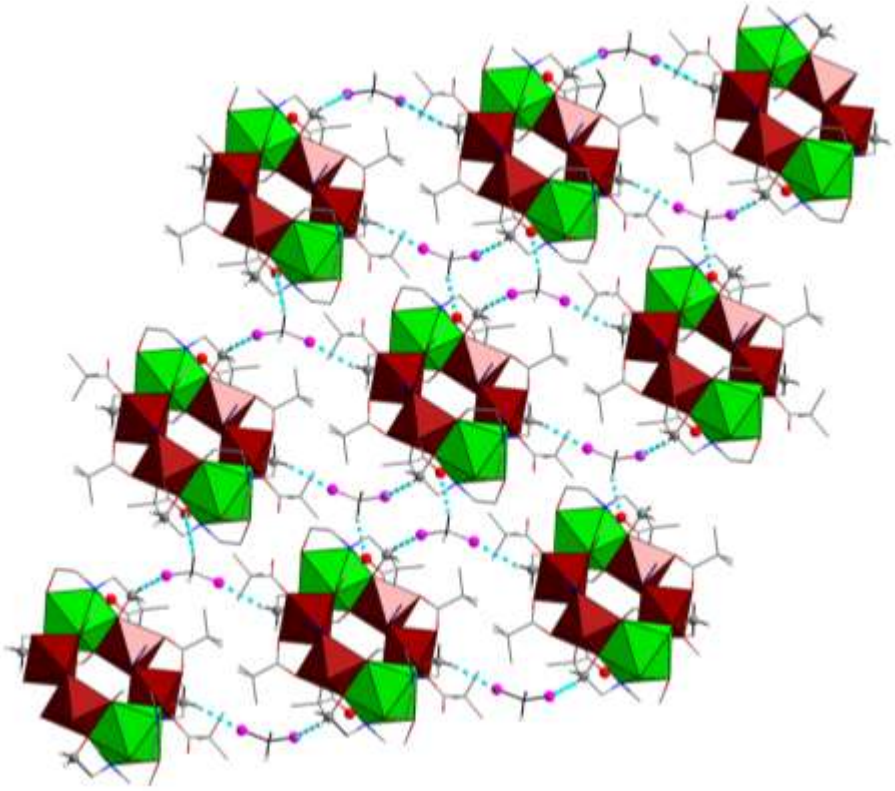

Figure S13. 2D layer formed through C–H…Cl and C–H…O interactions in structure **2a**/**b**. Hydrogen bonds are shown as dashed blue lines. All other hydrogen atoms (except those that participate in the formation of hydrogen bonds) are omitted for clarity. Color scheme: Ln, green; Fe, brown polyhedra; O, red; N, blue; C, gray sticks; Cl, pink spheres.

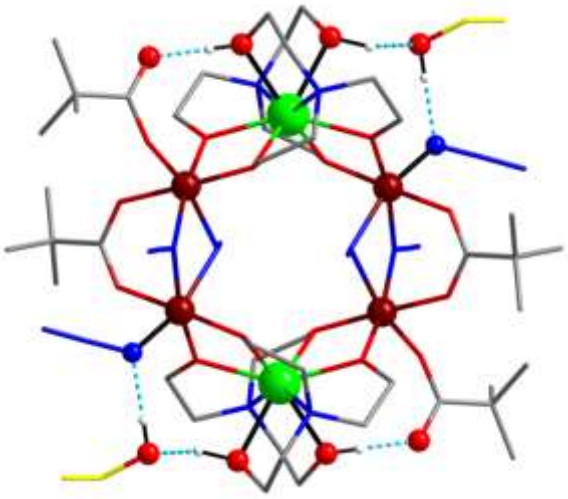

Figure S14. Intramolecular and intermolecular O–H···O and O–H···N hydrogen bonds (dashed blue lines) formed in compounds **3a** and **3b**. All other hydrogen atoms (except those that participate in the formation of hydrogen bonds) are omitted for clarity. Color scheme: Ln, green; Fe, brown spheres; O, red; N, blue; C, gray sticks. Oxygen and nitrogen atoms that form hydrogen bonds are shown as red and blue spheres, respectively. Solvent ethanol molecules are highlighted in yellow.

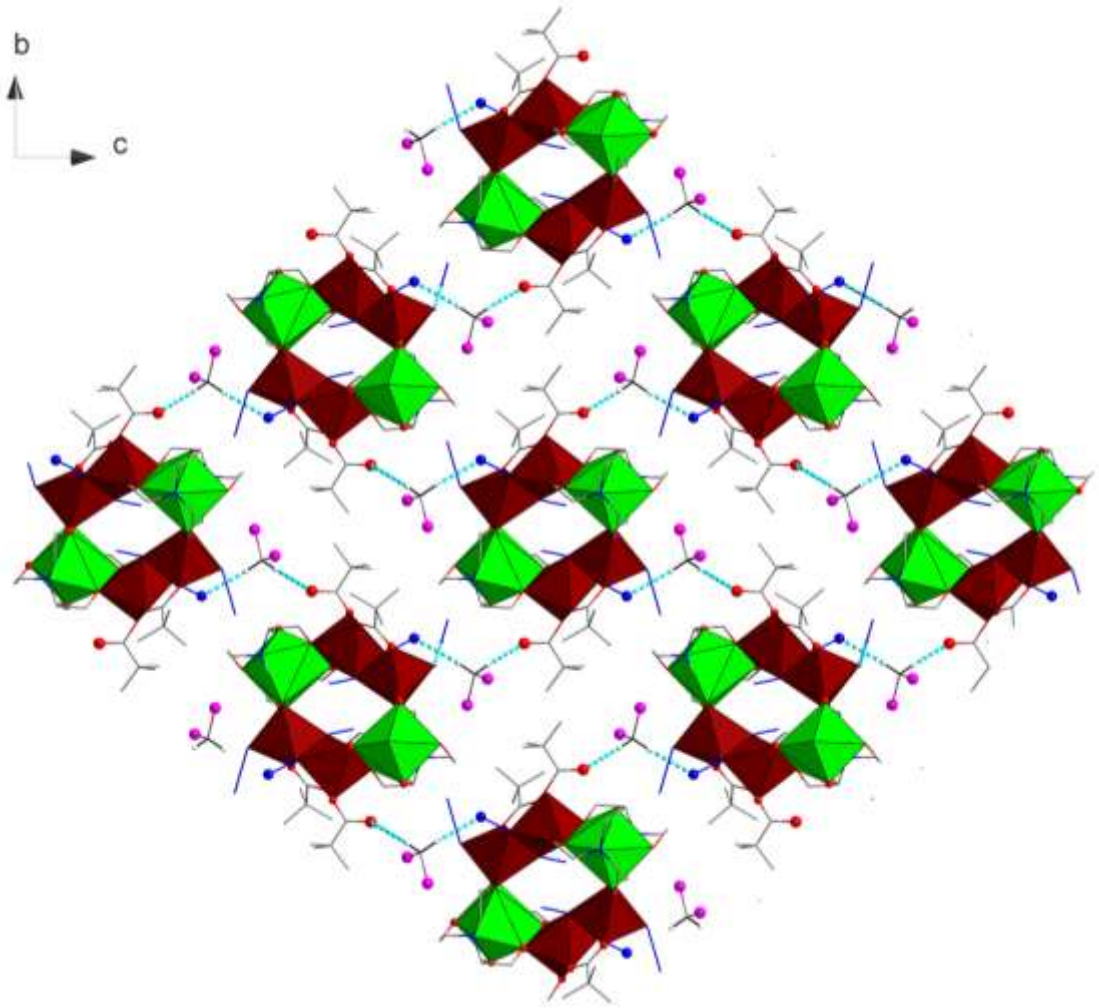

Figure S15. 2D layer formed in compounds **3a** and **3b** through C–H…O and C–H…N interactions between CH atom from CH_2Cl_2 and an uncoordinated O carboxylate atom and N atom of azide, respectively. The intermolecular hydrogen bonds shown as dashed blue lines. All other hydrogen atoms (except those that participate in the formation of hydrogen bonds) are omitted for clarity. Color scheme: Ln, green; Fe, brown polyhedra; O, red; N, blue; C, gray sticks; Cl, pink spheres. Oxygen and nitrogen atoms that form hydrogen bonds are shown as red and blue spheres, respectively. Solvent ethanol molecules are omitted for clarity.

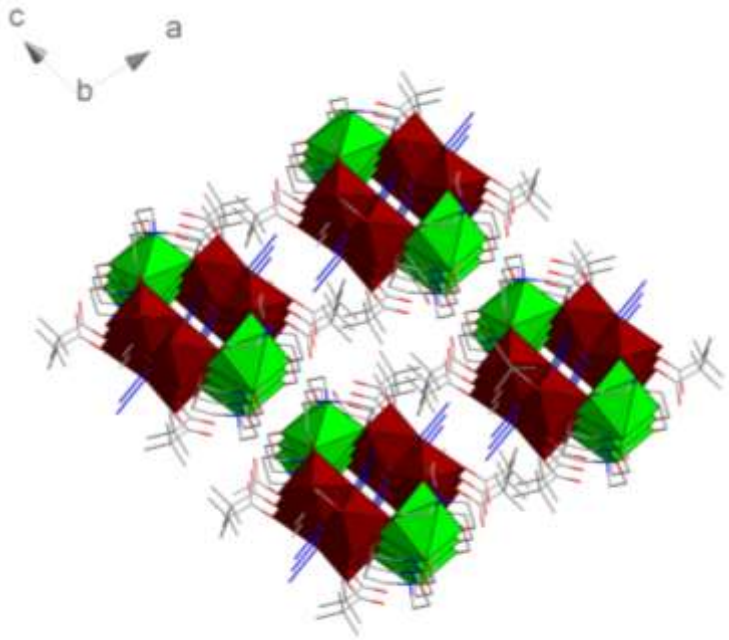

Figure S16. The stacked packing of {Fe_4Ln_2} wheels in compounds **1a/b/c** and **2a/b**. The viewing direction is approximately along the *b* axis. Coordination environment around metal atoms are shown as green (Ln) and brown (Fe) polyhedra, N: blue, O: red, C: grey sticks. Hydrogen atoms and solvent ethanol molecules are omitted for clarity.

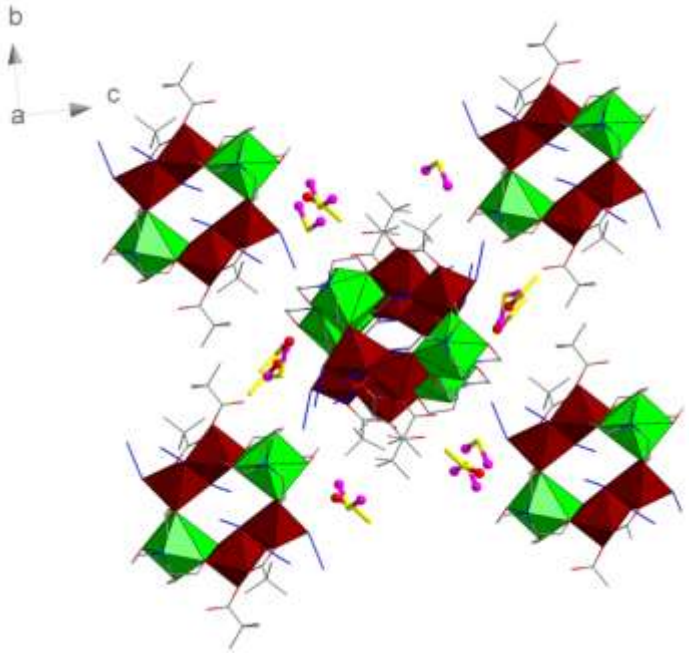

Figure S17. The stacked packing of {Fe_4Ln_2} wheels in compounds **3a/b**. The viewing direction is approximately along the *a* axis. Coordination environment around metal atoms are shown as green (Ln) and brown (Fe) polyhedra, N: blue, O: red, C: gray sticks. Hydrogen atoms and are omitted for clarity. In solvent ethanol and dichloromethane molecule atoms are highlighted: C atoms, yellow sticks; O atoms, red spheres; Cl atoms, pink spheres.

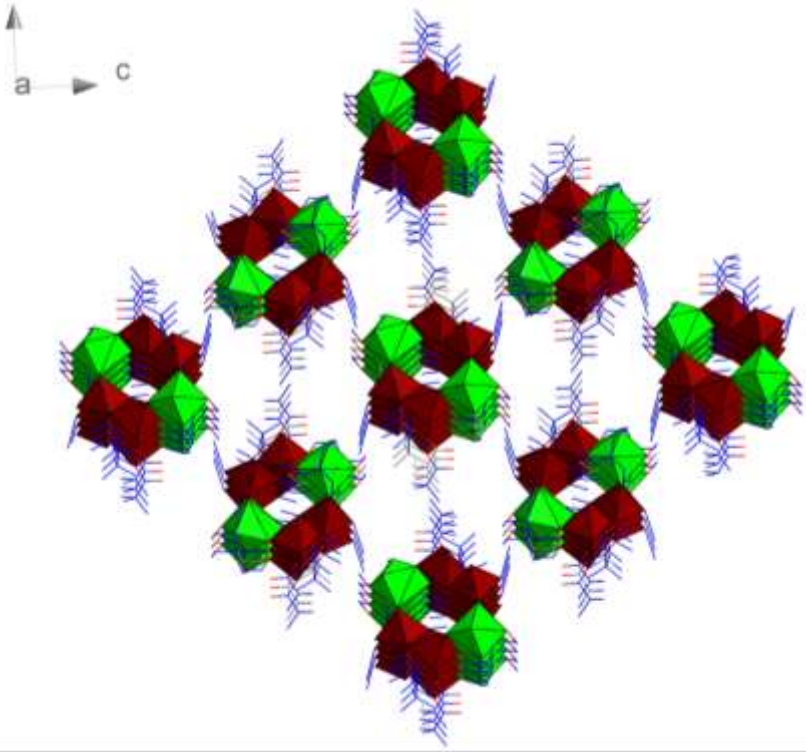

Figure S18. Packing diagram in compounds **3a/b** showing the alternating orientation of the stacked {Fe_4Ln_2} wheels. Coordination environment around metal atoms are shown as green (Ln) and brown (Fe) polyhedra, N: blue, O: red, C: gray sticks. Hydrogen atoms and solvent ethanol and dichloromethane molecules are omitted for clarity.

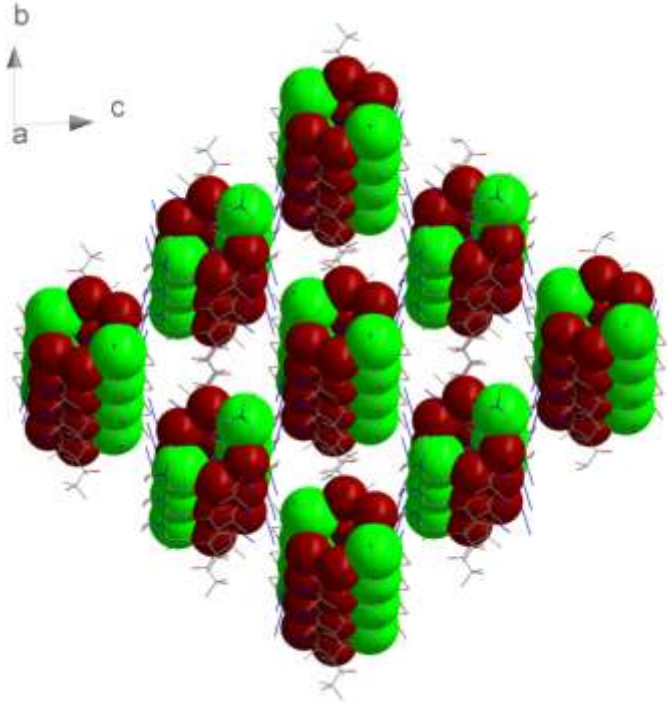

Figure S19. Space-filling representation of packing diagram showing the formation of columns from {Fe_2Ln_2} wheels in compounds **3a/b**. Only metal atoms are shown in space-filling mode (Ln: green, Fe: brown). Other atoms are shown as sticks N: blue, O: red, C: gray. Hydrogen atoms and solvent ethanol and dichloromethane molecules are omitted for clarity.

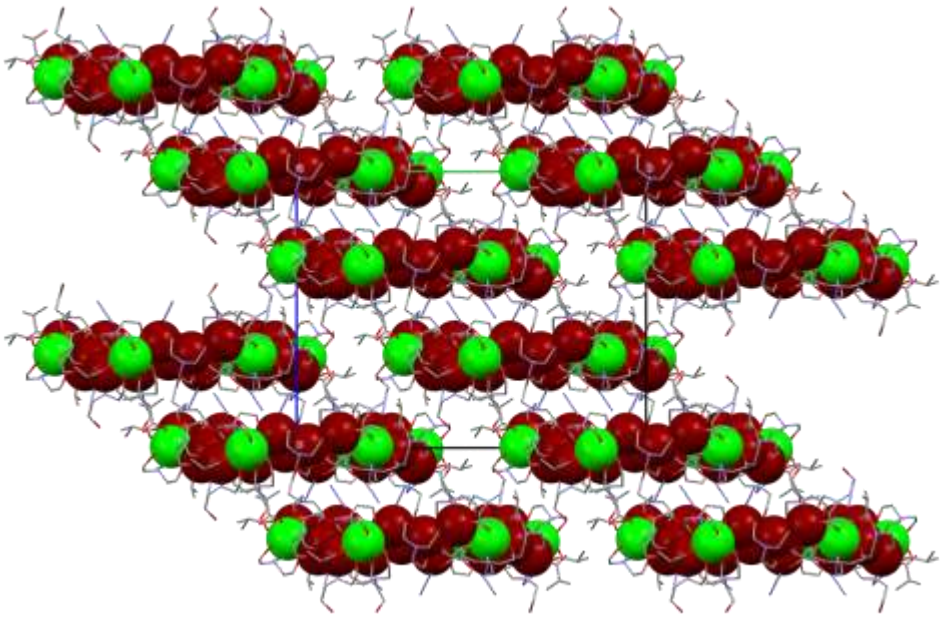

Figure S20. A view of $\{Fe_{18}M_6\}$ (M^{3+} = Dy, Sm) rings in compounds **4a** and **8** along the *a* axis. Metal atoms have space-filling mode and highlighted in green (M) and brown (Fe) and other atoms are shown as sticks N: blue, O: red, C: grey sticks. Hydrogen atoms and solvent molecules are omitted for clarity.

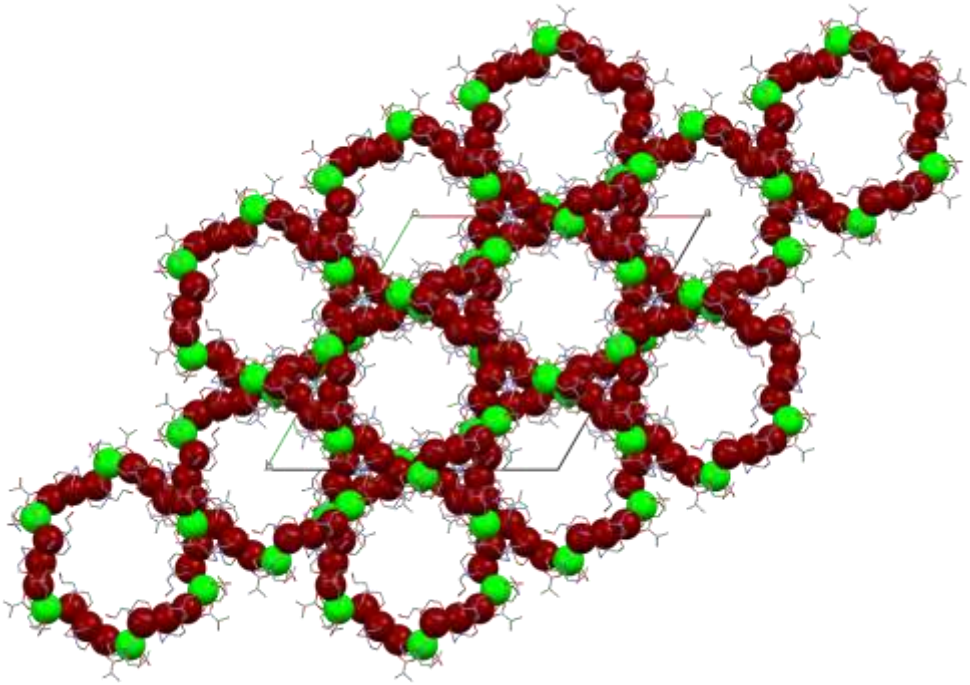

Figure S21. A view of $\{Fe_{18}M_6\}$(M^{3+} = Dy, Sm) rings in compounds **4a** and **8** along the *c* axis. Only metal atoms have space-filling mode and highlighted in green (M) and brown (Fe). Other atoms are shown as sticks N: blue, O: red, C: grey sticks. Hydrogen atoms and solvent molecules are omitted for clarity.

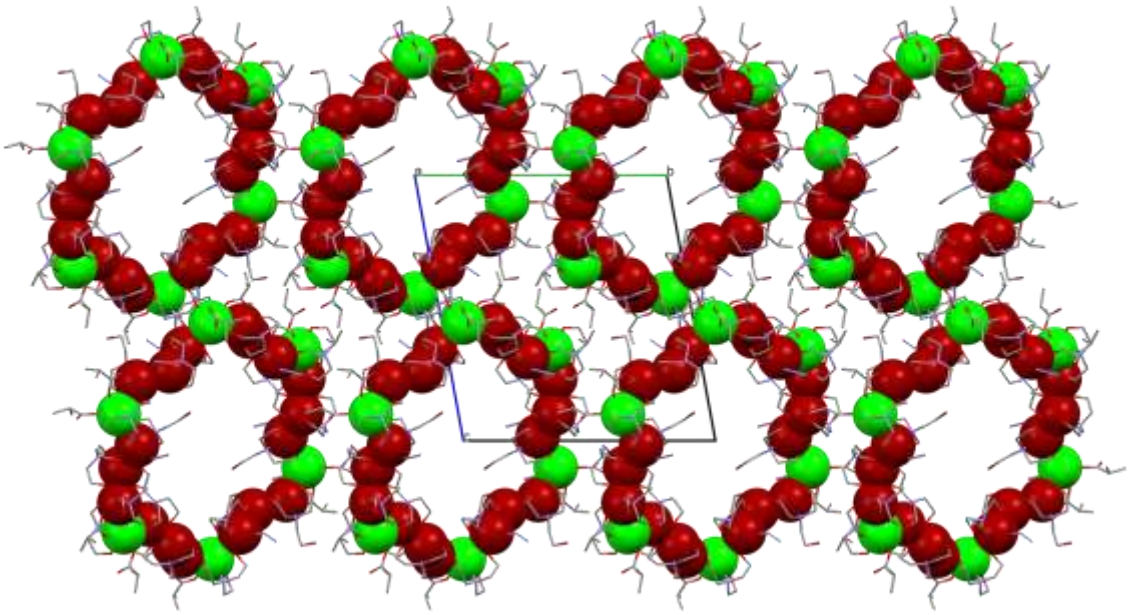

Figure S22. A view of $\{Fe_{18}M_6\}$ rings in compounds **4-10** (except **4a** and **8**) along the *a* axis. Only metal atoms have space-filling mode and highlighted in green (M) and brown (Fe). Other atoms are shown as sticks N: blue, O: red, C: grey sticks. Hydrogen atoms and solvent molecules are omitted for clarity.

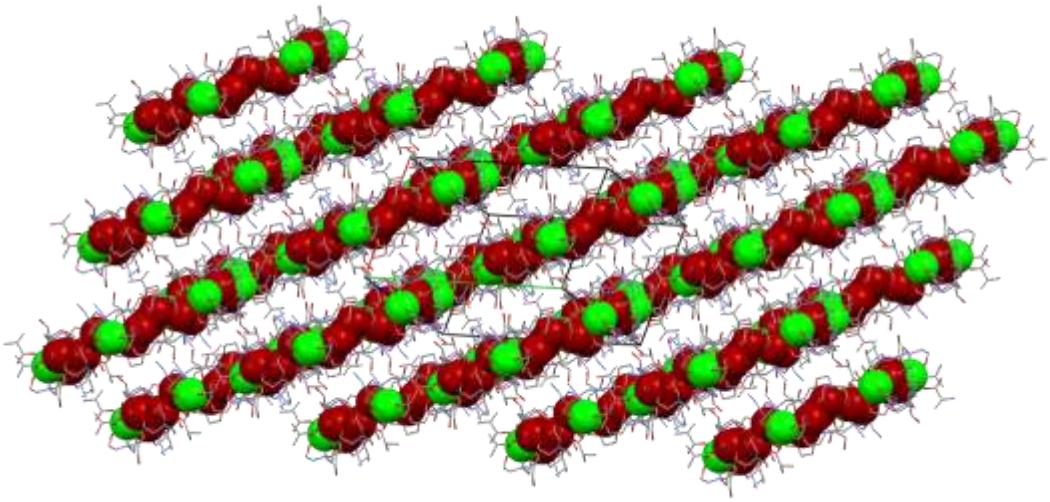

Figure S23. Packing diagram of **4-10** (except **4a** and **8**). Only metal atoms have space-filling mode and highlighted in green (M) and brown (Fe). Other atoms are shown as sticks N: blue, O: red, C: grey sticks. Hydrogen atoms and solvent molecules are omitted for clarity.

TGA data

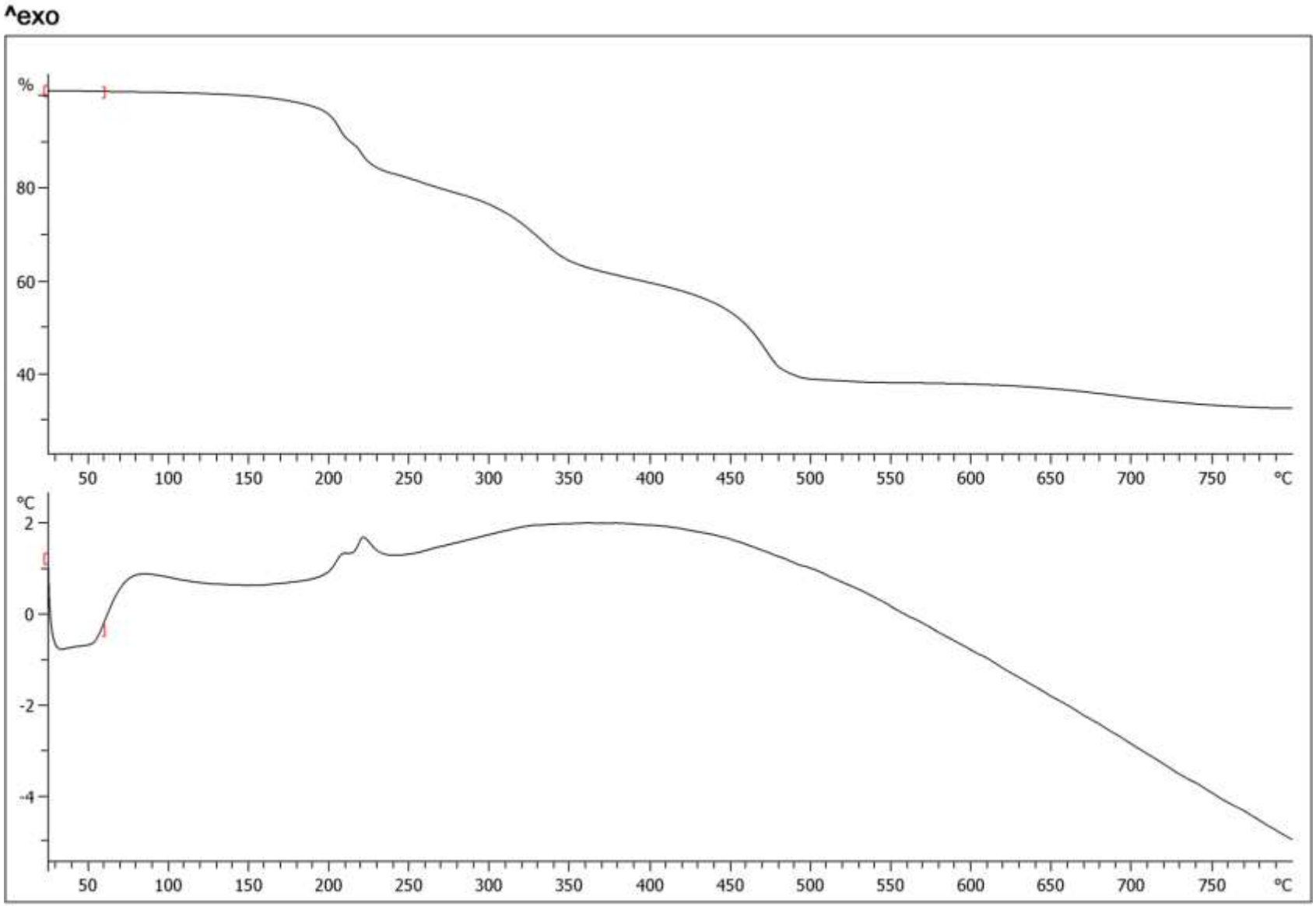

Figure S24. TGA/DTA curves for $[Fe_4Dy_2(O_2CCMe_3)_6(N_3)_4(Htea)_4]\cdot 2(EtOH)$ (**1a**).

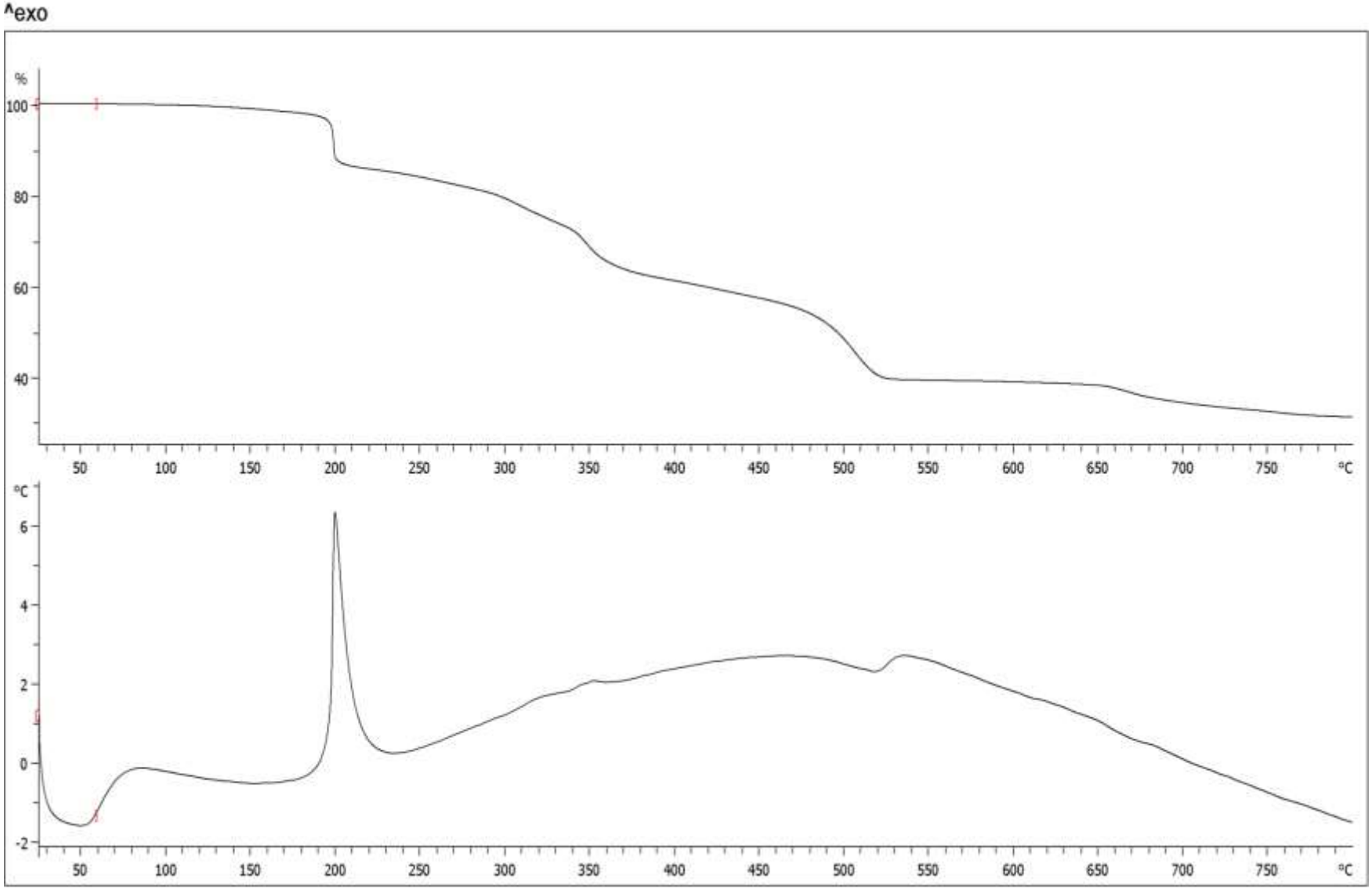

Figure S25. TGA/DTA curves for $[Fe_4Er_2(O_2CCMe_3)_6(N_3)_4(Htea)_4]\cdot 2(EtOH)$ (**1b**).

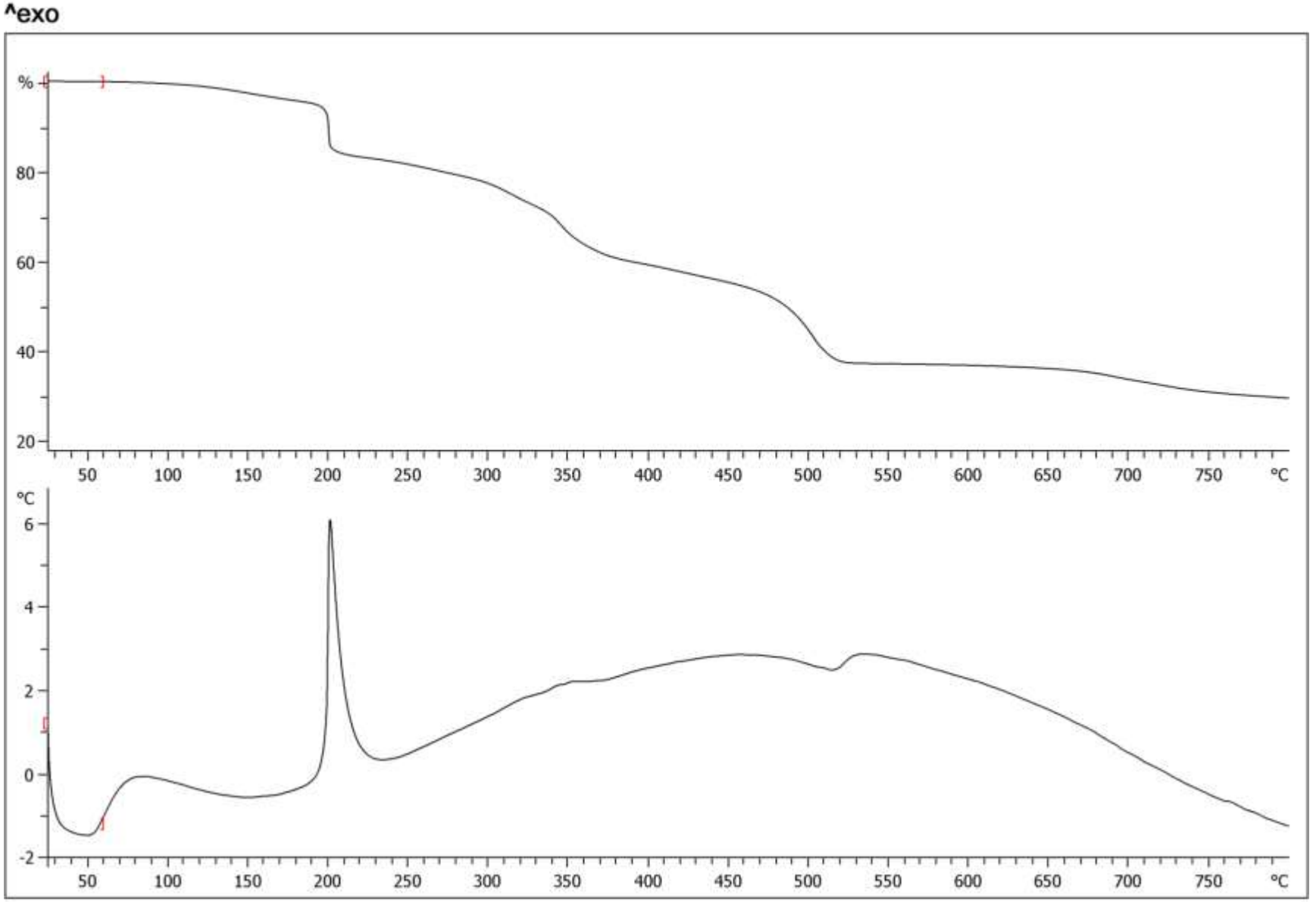

Figure S26. TGA/DTA curves for $[Fe_4Ho_2(O_2CCMe_3)_6(N_3)_4(Htea)_4]\cdot 2(EtOH)$ (**1c**).

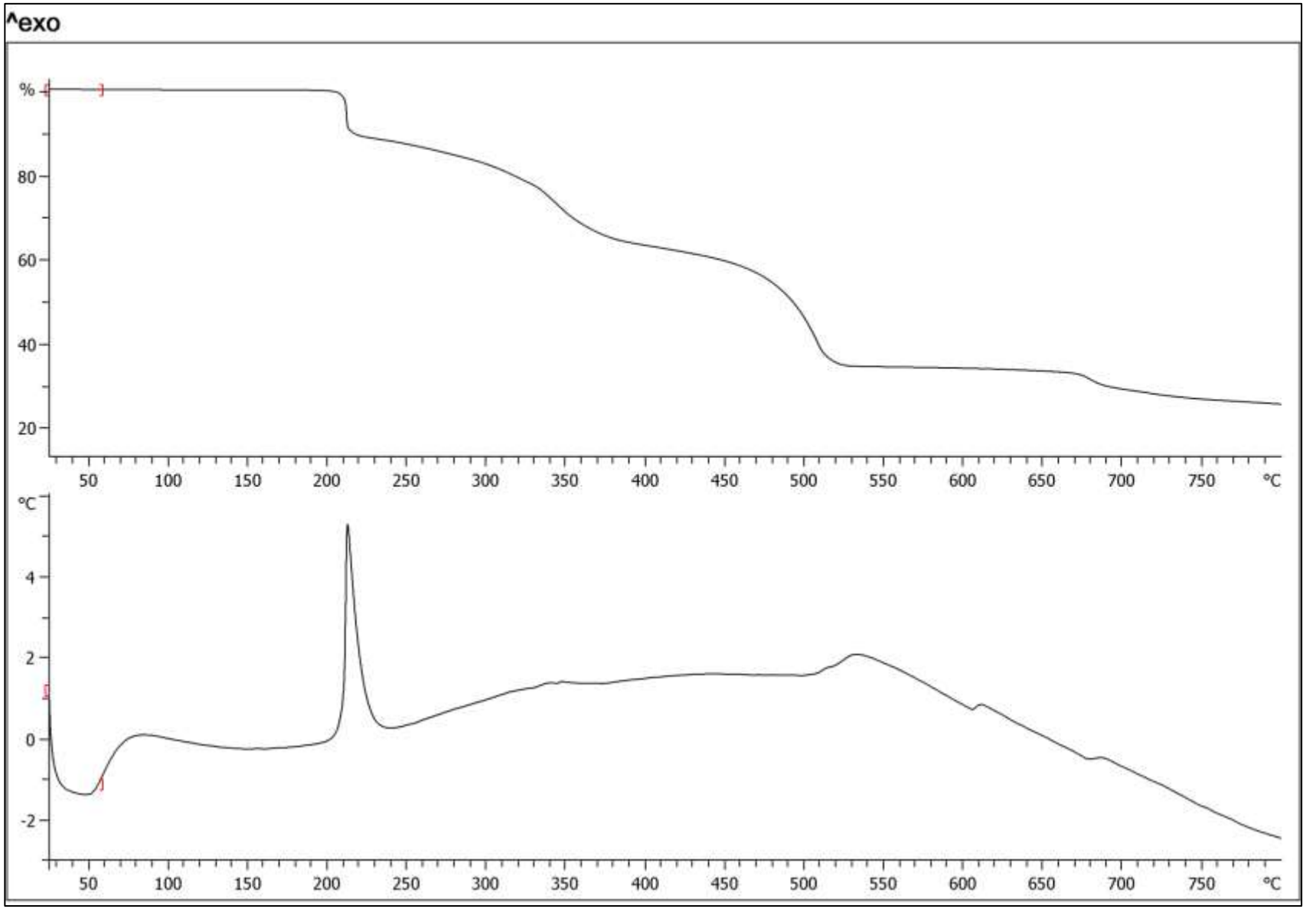

Figure S27. TGA/DTA curves for $[Fe_4Dy_2(O_2CCMe_3)_6(N_3)_4(Htea)_4]\cdot 2(CH_2Cl_2)$ (**2a**).

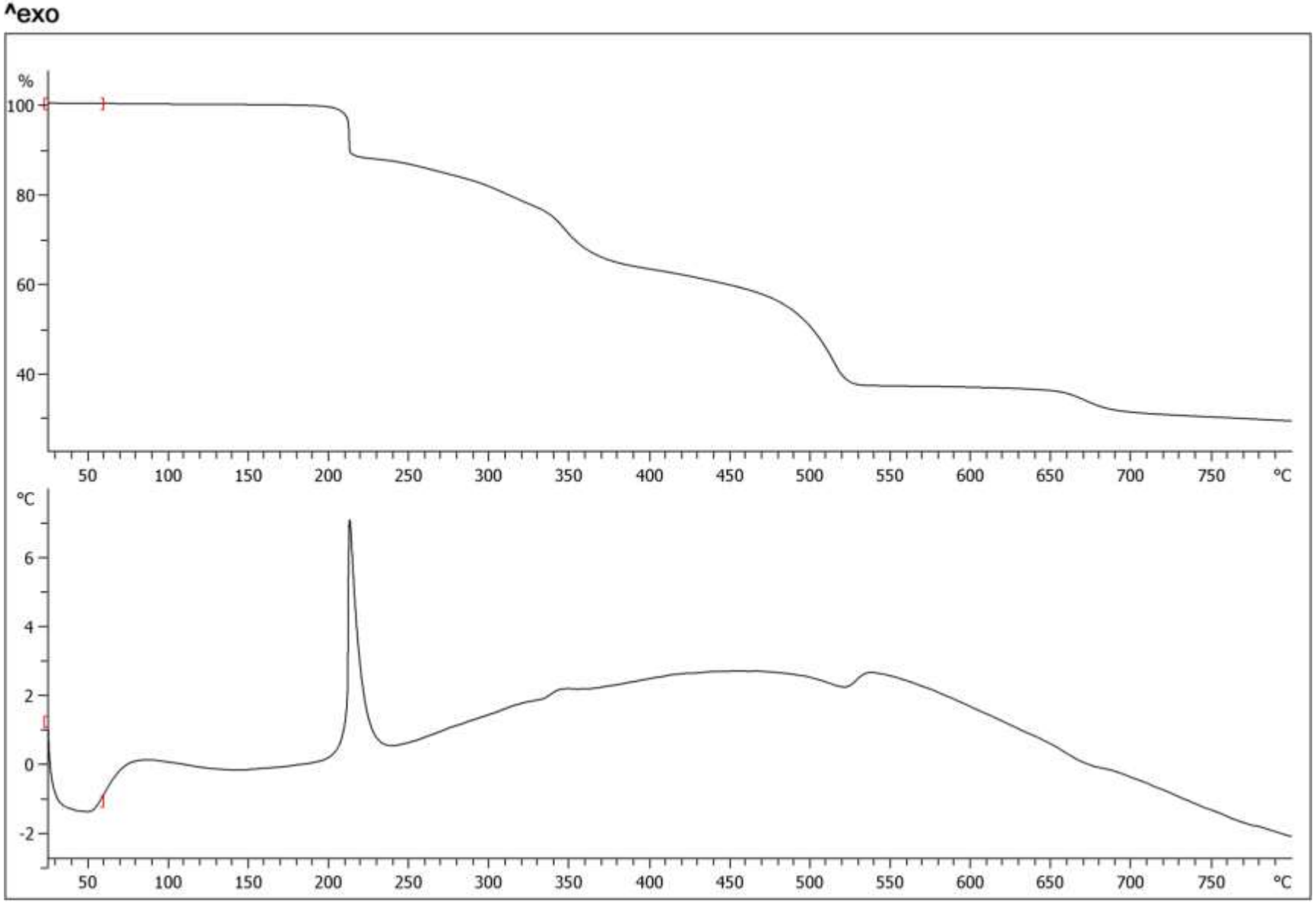

Figure S28. TGA/DTA curves for $[Fe_4Er_2(O_2CCMe_3)_6(N_3)_4(Htea)_4]\cdot 2(CH_2Cl_2)$ (**2b**).

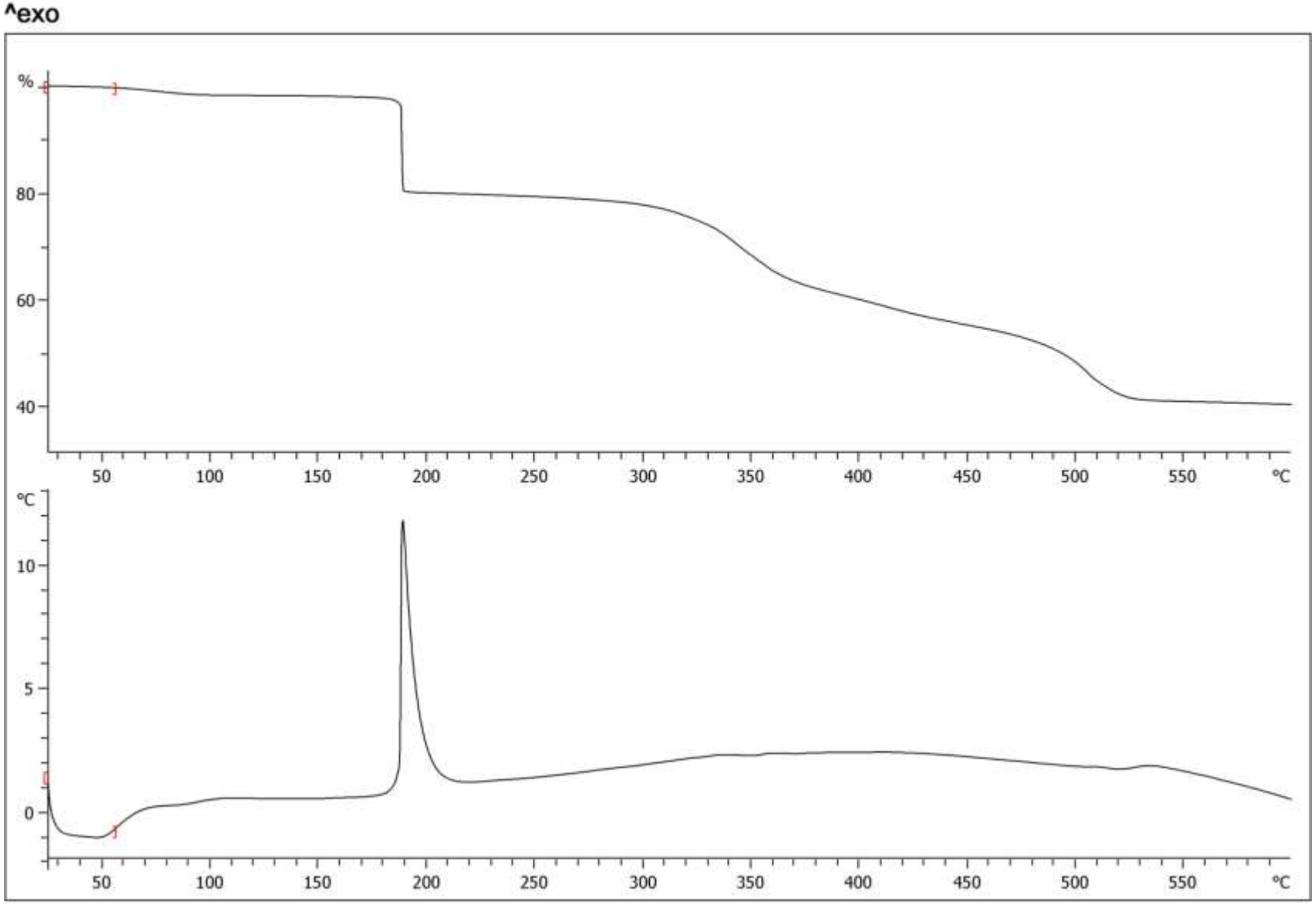

Figure S29. TGA/DTA curves for $[Fe_4Dy_2(O_2CCMe_3)_4(N_3)_6(Htea)_4]\cdot 2(CH_2Cl_2)\cdot 2(EtOH)$ (**3a**)

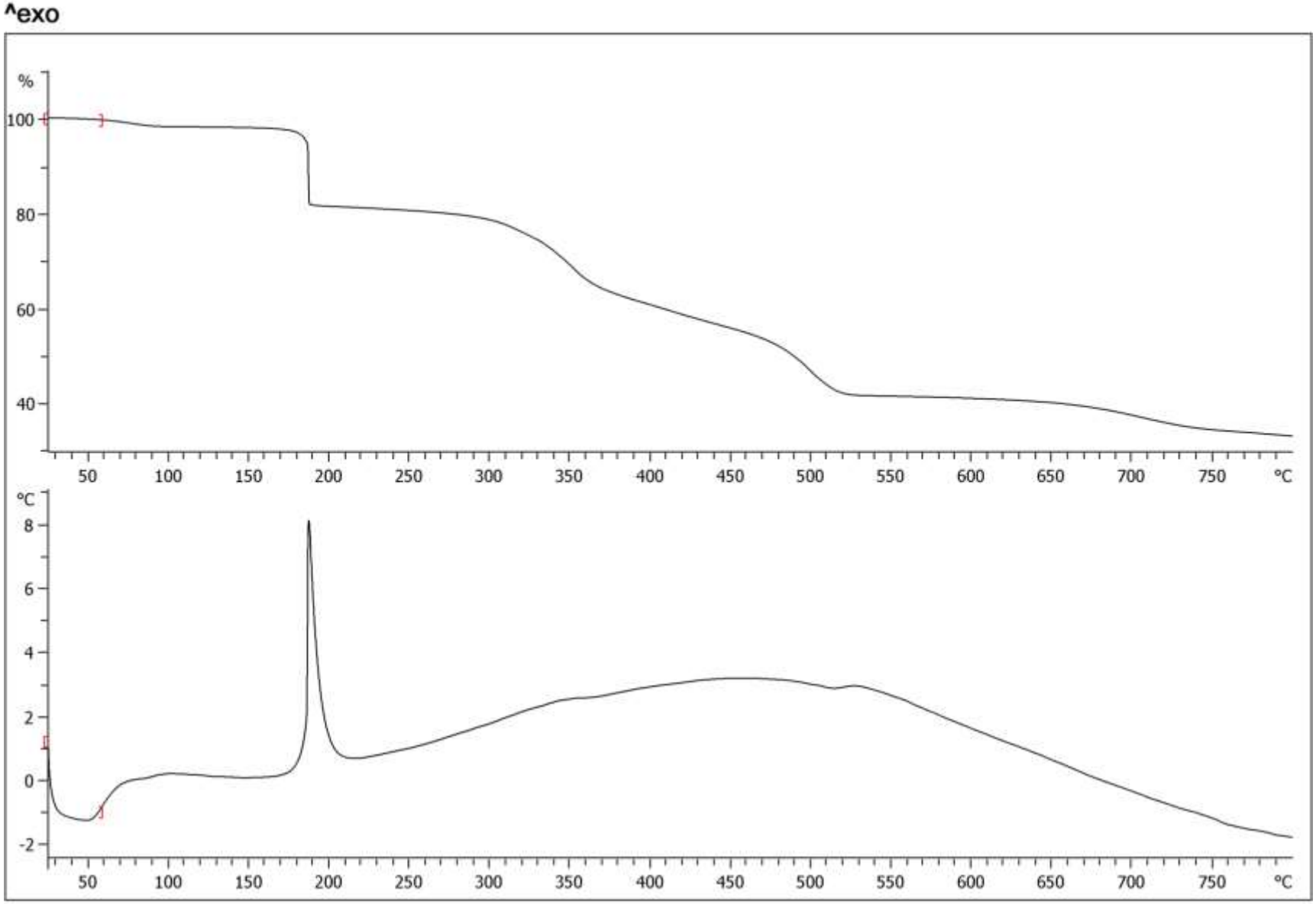

Figure S30. TGA/DTA curves for $[Fe_4Er_2(O_2CCMe_3)_4(N_3)_6(Htea)_4]\cdot 2(CH_2Cl_2)\cdot 2(EtOH)$ (**3b**).

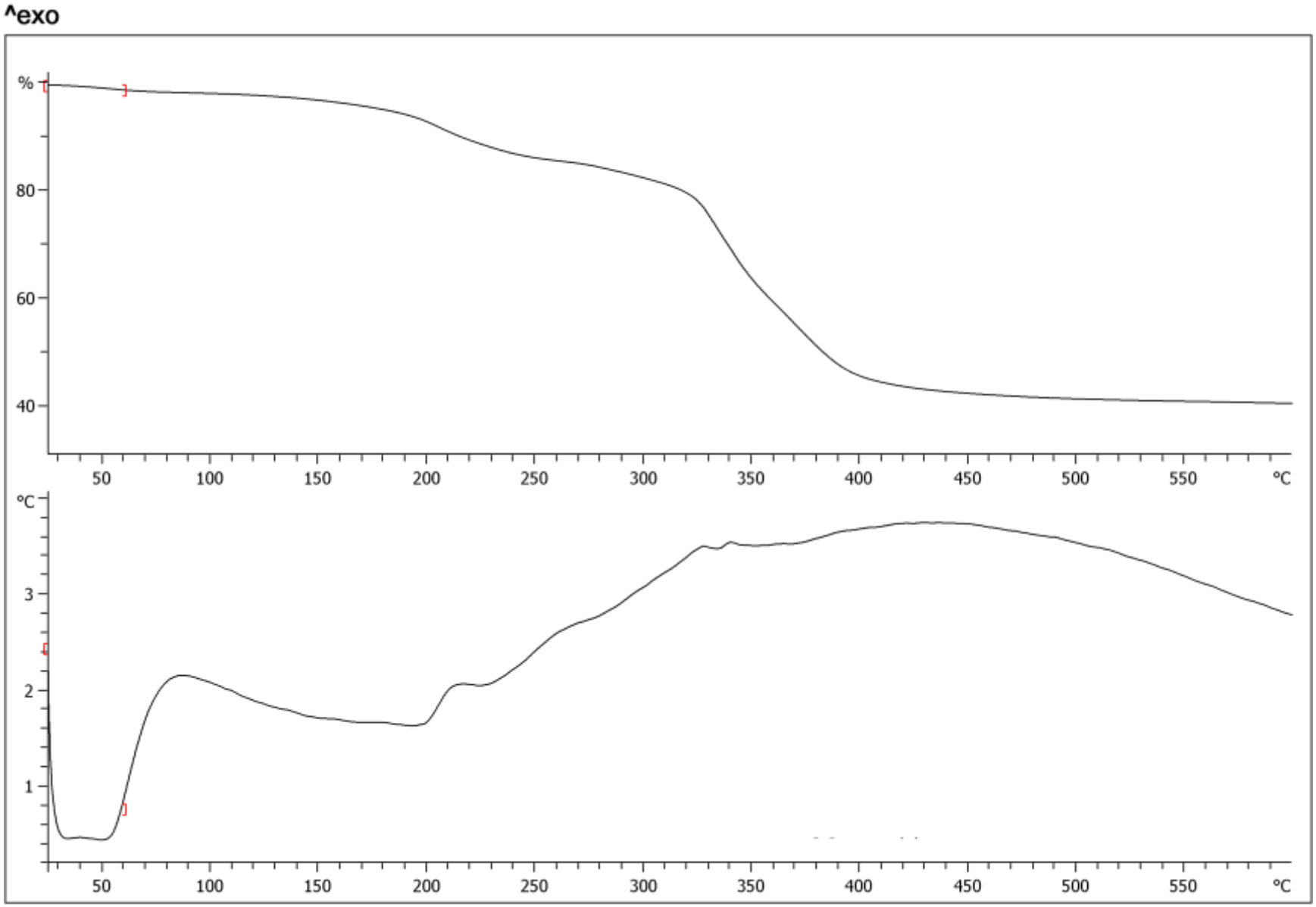

Figure S31. TGA/DTA curves for ($[Fe_{18}Dy_6(O_2CCHMe_2)_{12}(Htea)_{18}(tea)_6(N_3)_6]\cdot n$(solvent) (**4**).

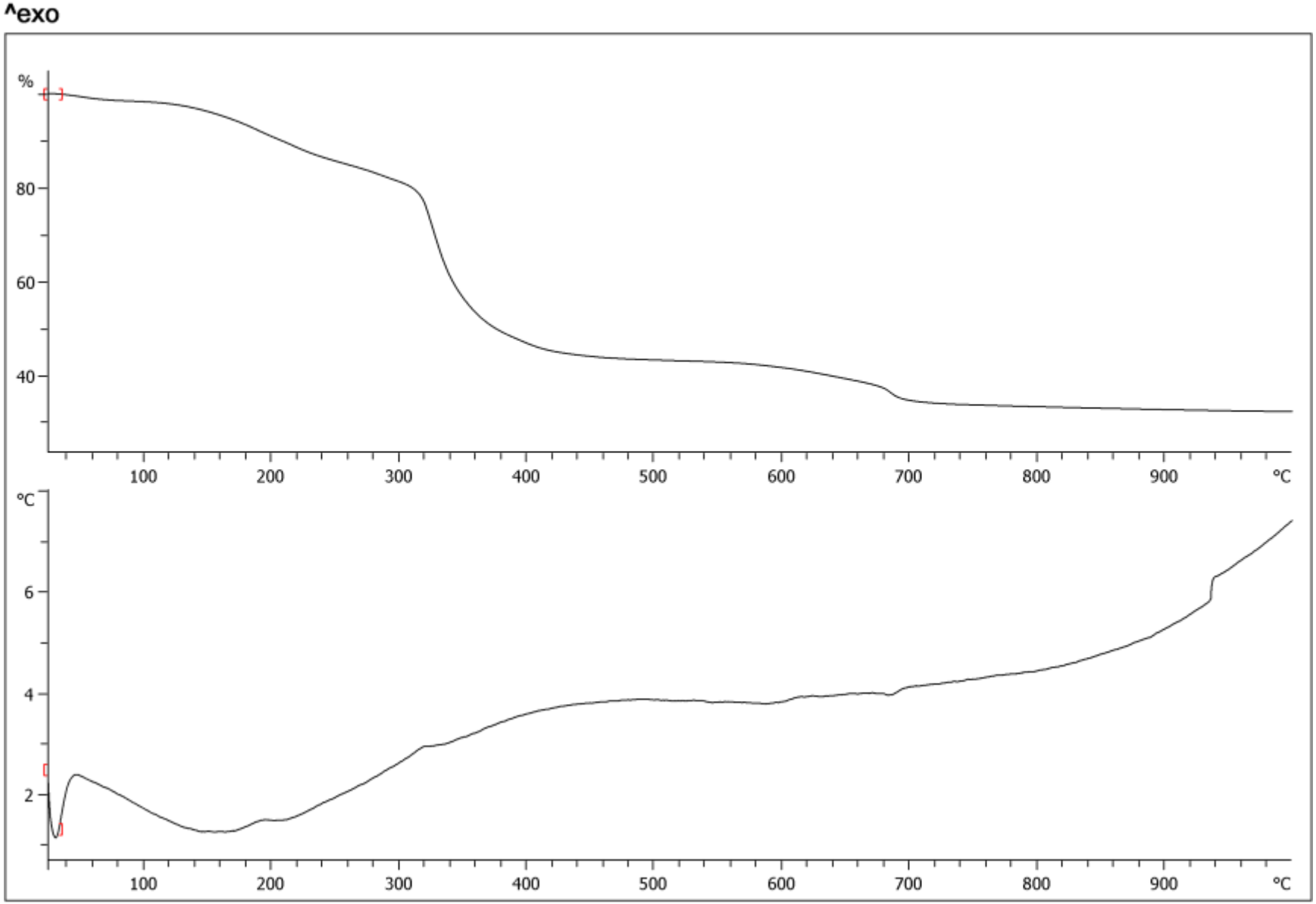

Figure S32. TGA/DTA curves for ($[Fe_{18}Dy_6(O_2CCHMe_2)_{12}(Htea)_{18}(tea)_6(N_3)_6]\cdot n$(solvent) (**4a**).

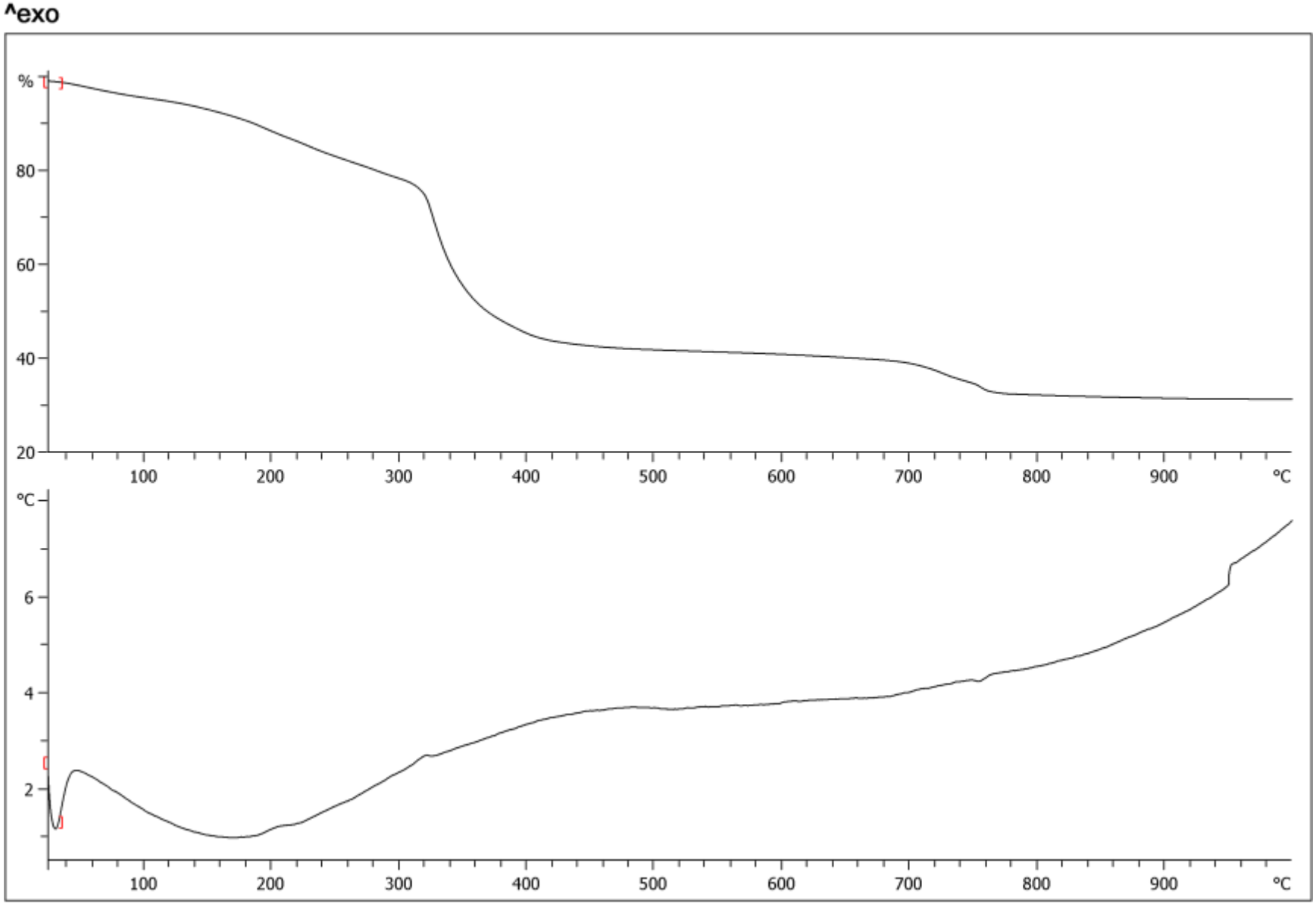

Figure S33. TGA/DTA curves for ($[Fe_{18}Gd_6(O_2CCHMe_2)_{12}(Htea)_{18}(tea)_6(N_3)_6]\cdot n$(solvent) (**5**).

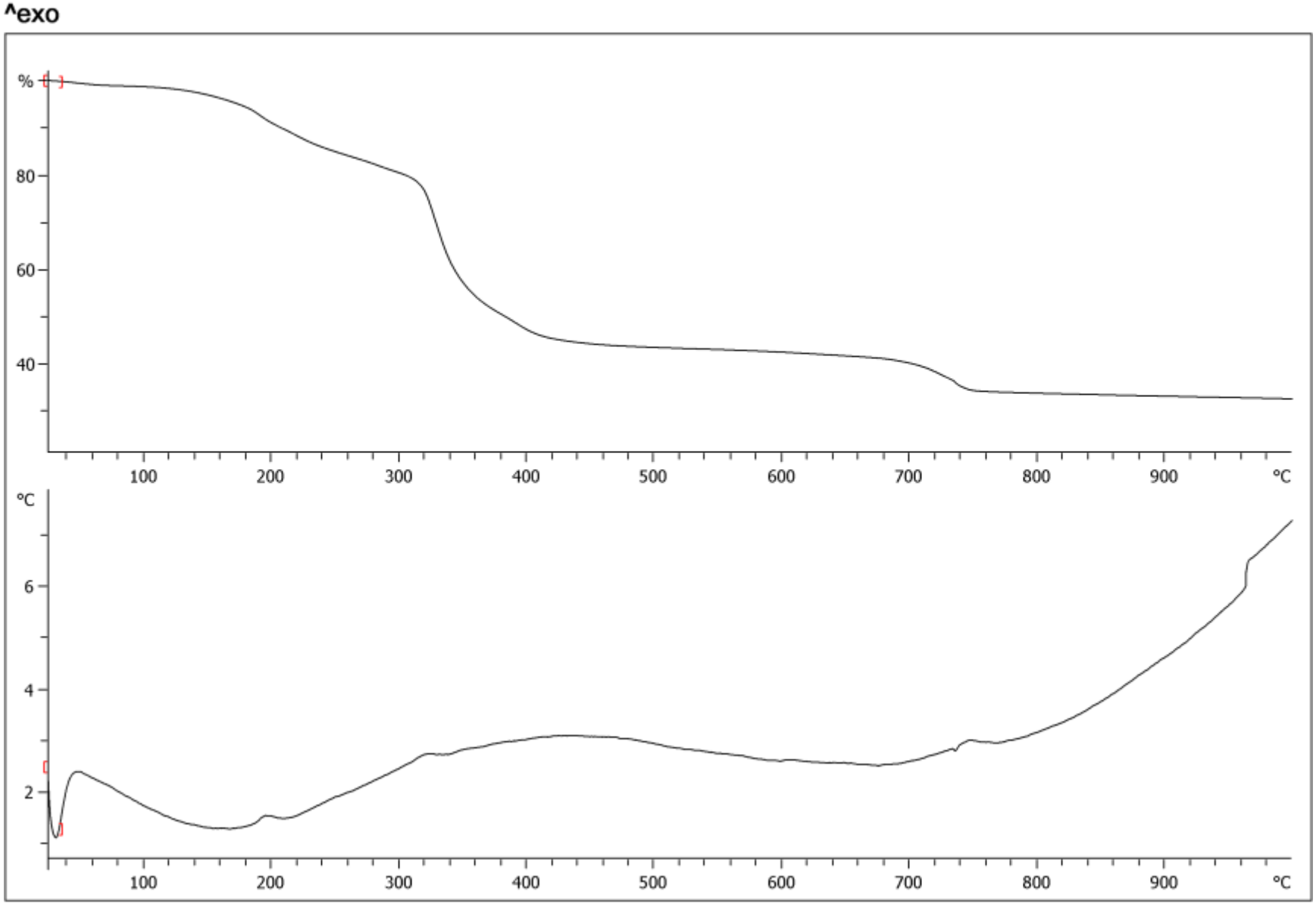

Figure S34. TGA/DTA curves for ($[Fe_{18}Tb_6(O_2CCHMe_2)_{12}(Htea)_{18}(tea)_6(N_3)_6]\cdot n$(solvent) (**6**).

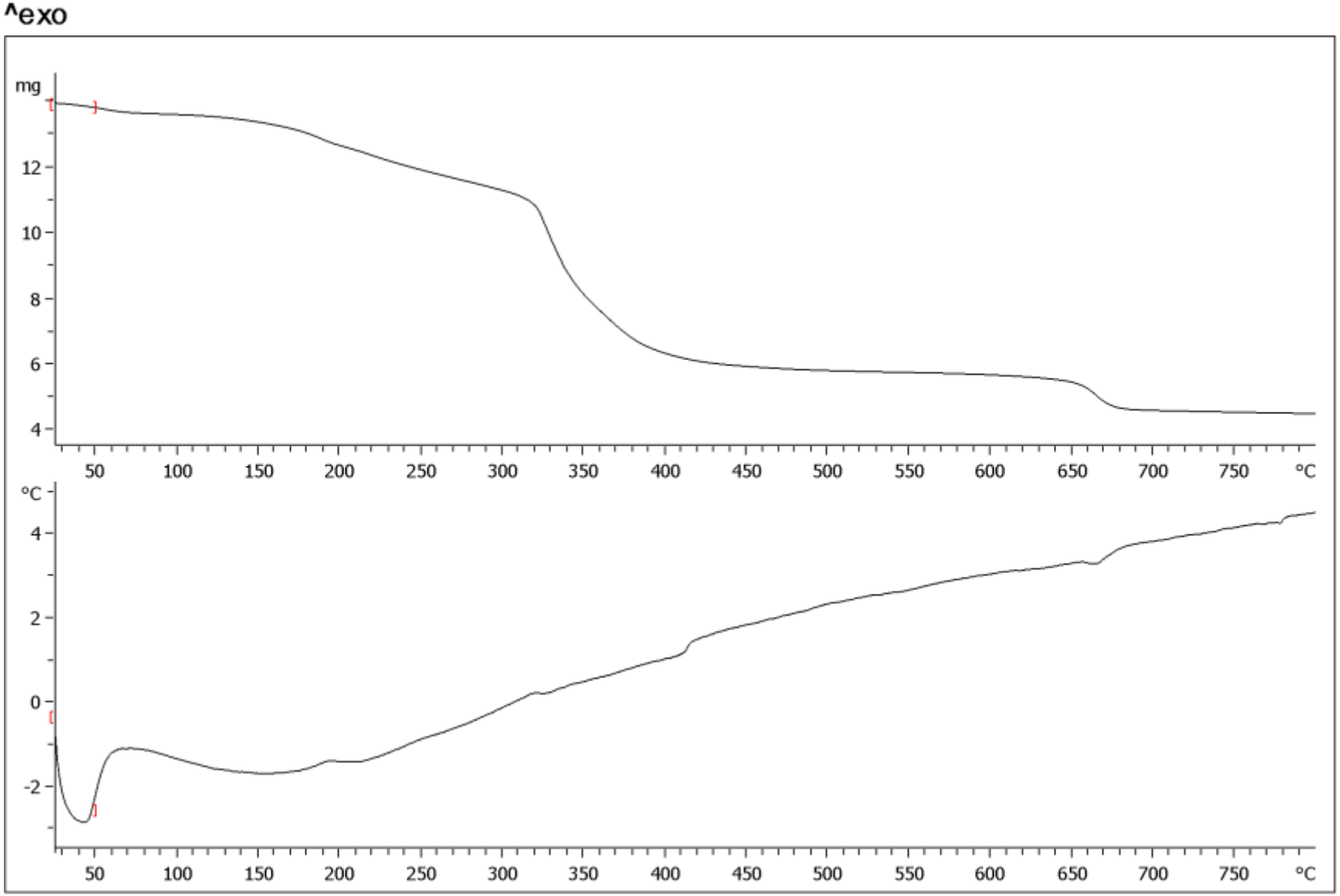

Figure S35. TGA/DTA curves for ($[Fe_{18}Ho_6(O_2CCHMe_2)_{12}(Htea)_{18}(tea)_6(N_3)_6]\cdot n$(solvent) (**7**).

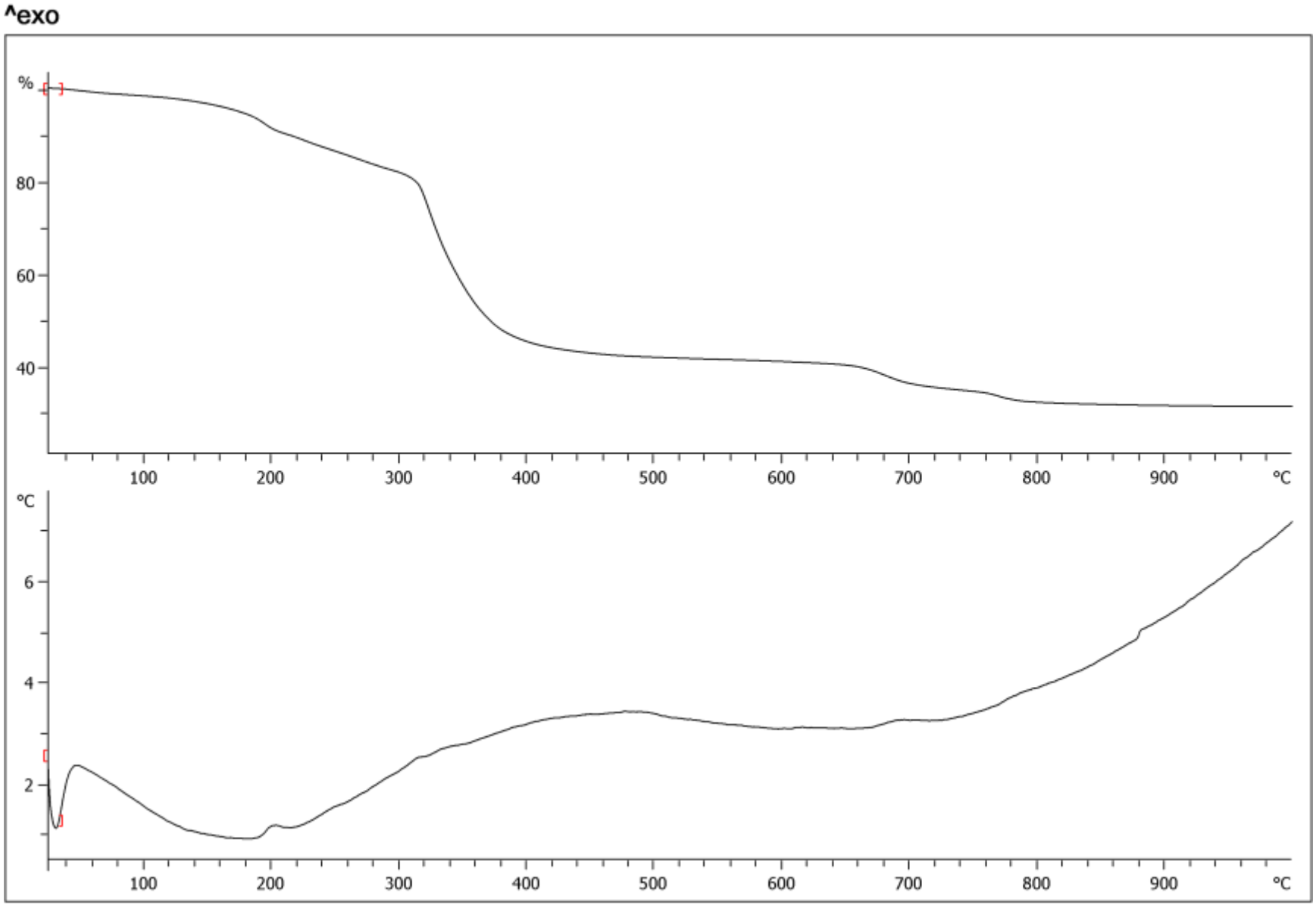

Figure S36. TGA/DTA curves for ([$Fe_{18}Sm_6(O_2CCHMe_2)_{12}(Htea)_{18}(tea)_6(N_3)_6$]·*n*(solvent) (**8**).

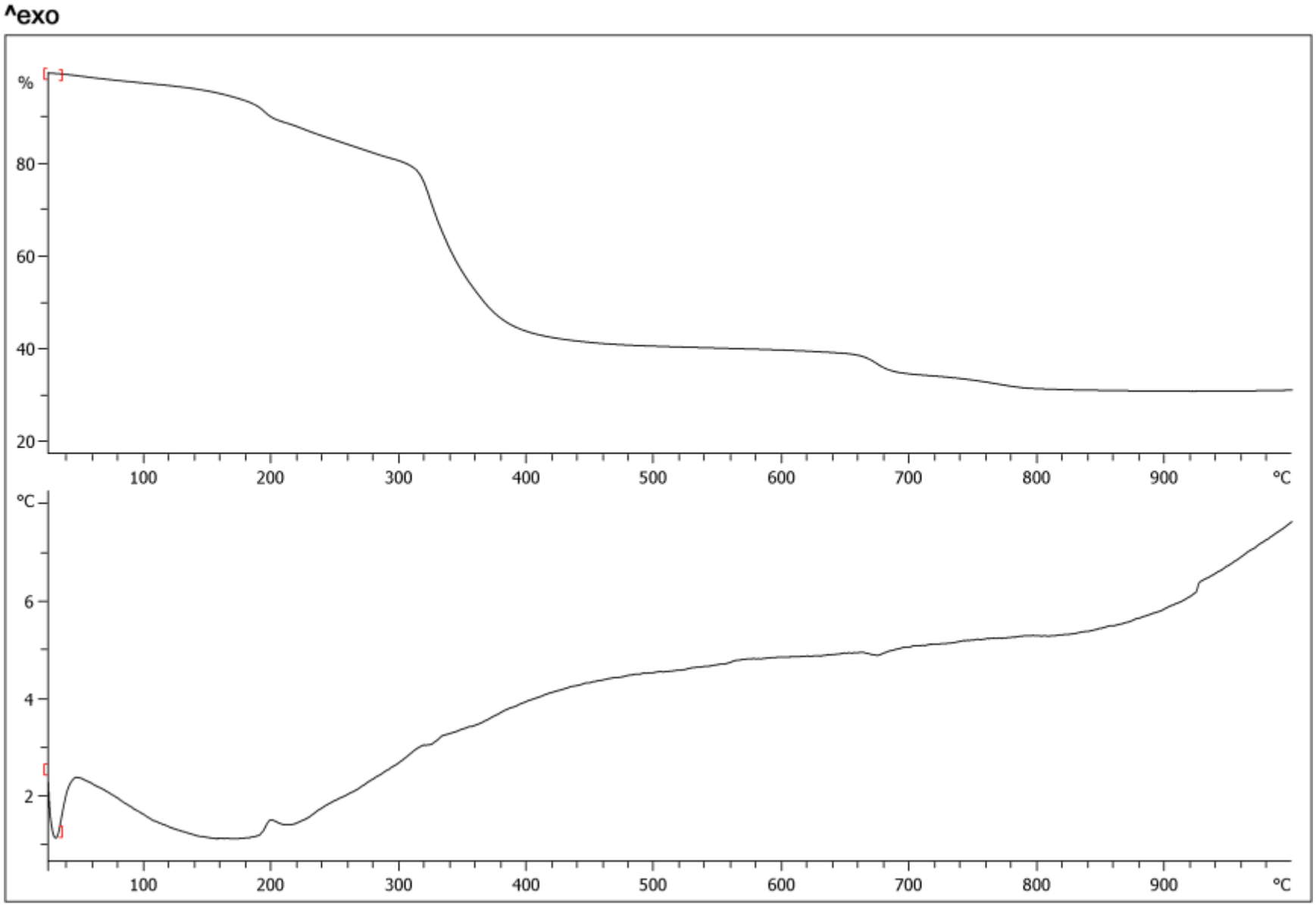

Figure S37. TGA/DTA curves for ($[Fe_{18}Eu_6(O_2CCHMe_2)_{12}(Htea)_{18}(tea)_6(N_3)_6]\cdot n$(solvent) (**9**).

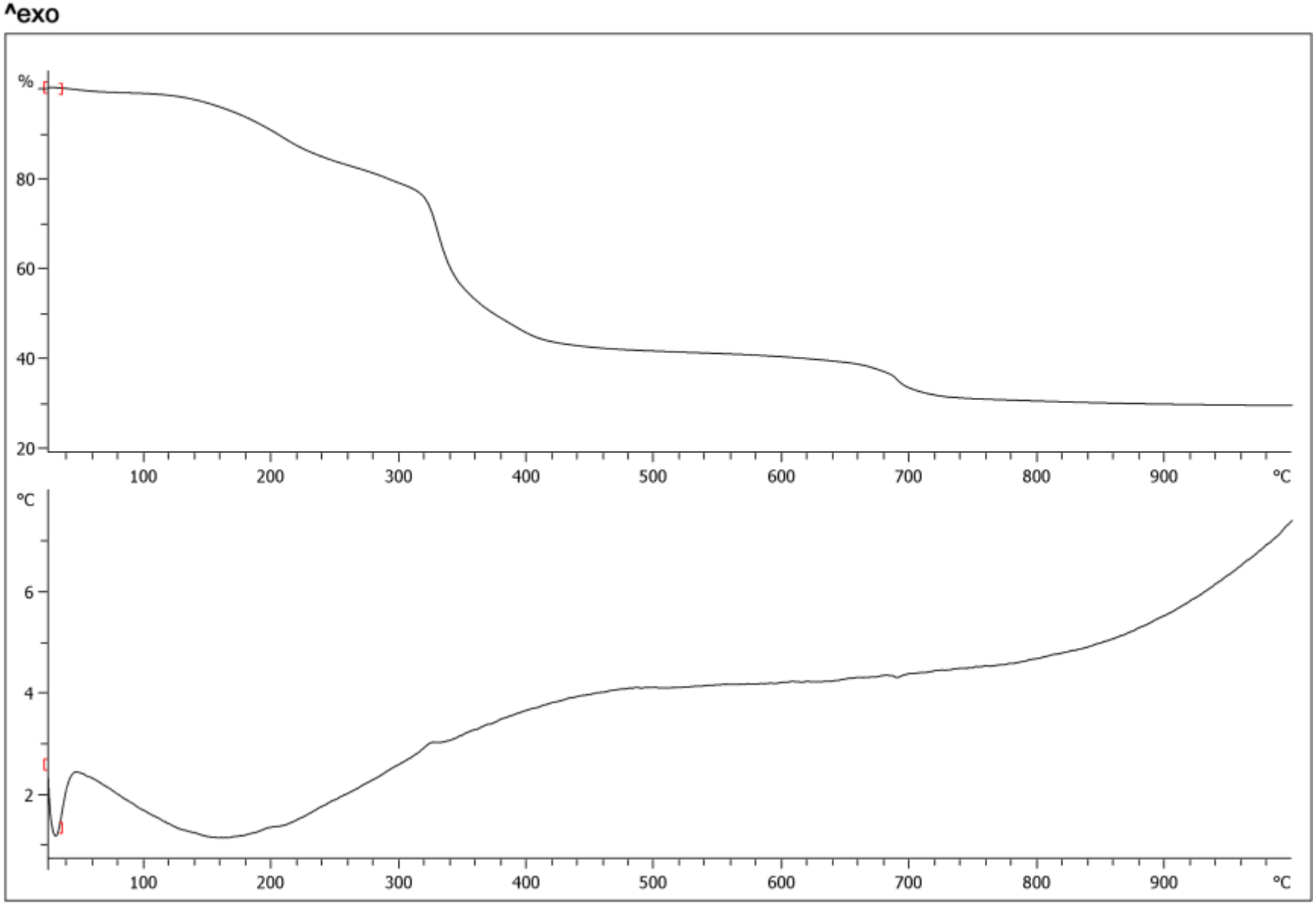

Figure S38. TGA/DTA curves for ($[Fe_{18}Y_6(O_2CCHMe_2)_{12}(Htea)_{18}(tea)_6(N_3)_6]\cdot n$(solvent) (**10**).

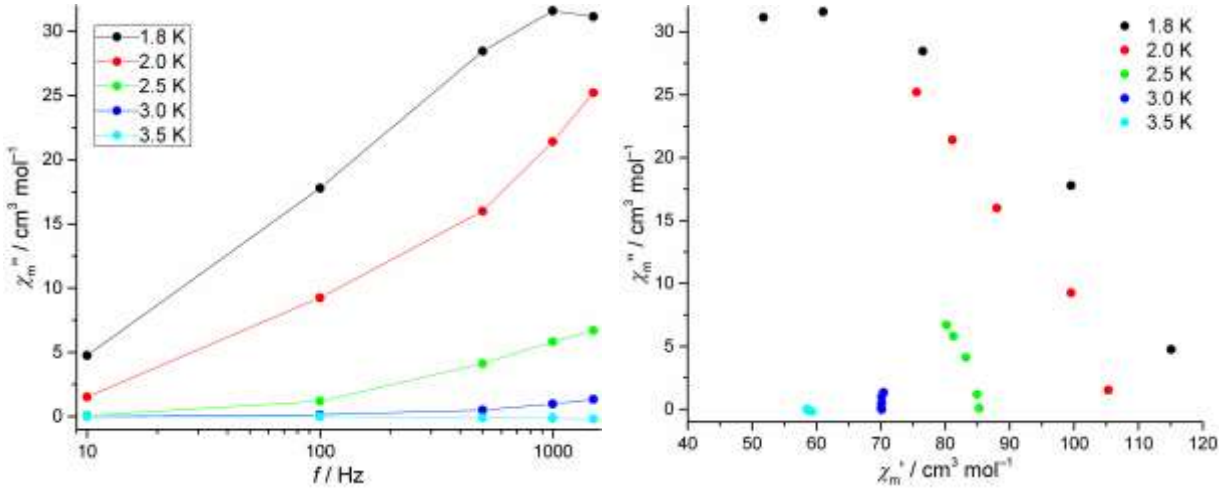

Figure S39. Left: out-of-phase magnetic susceptibility χ''_m vs. frequency f (lines are guidelines for the eyes); right: related Cole-Cole plot of **1c** in absence of a static field B.

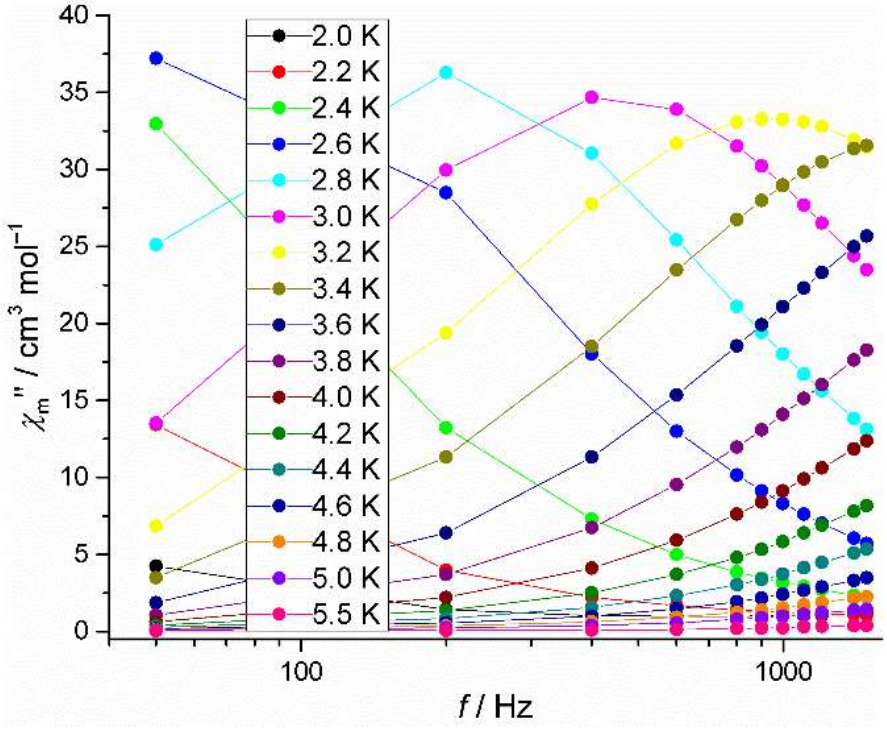

Figure S40. Out-of-phase magnetic susceptibility χ''_m vs. frequency f (50–1500 Hz) of **1d** in absence of a static field B (lines are guides to the eye).

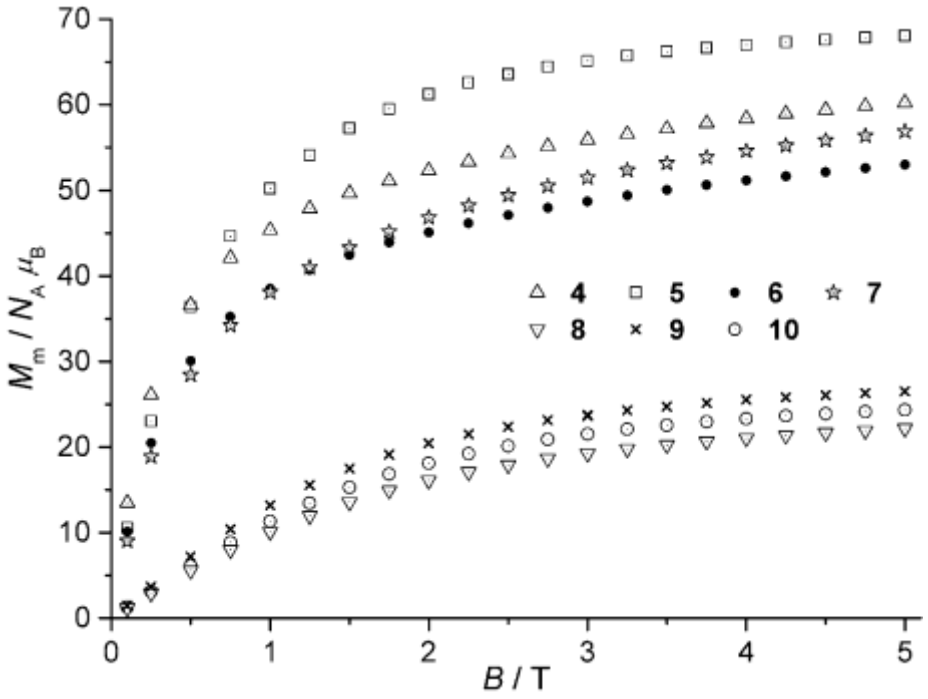

Figure S41. Dependence of the molar magnetization M_m on the applied field B at T = 2.0 K of **4**–**10.**

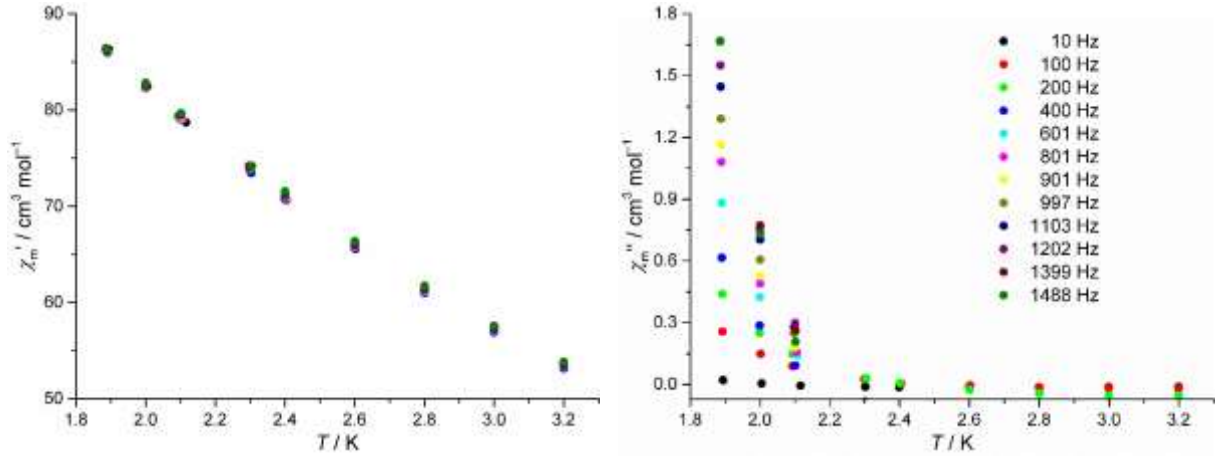

Figure S42. Temperature dependence of in-phase χ'_m and out-of-phase magnetic susceptibility χ''_m of **4** in absence of a static field B.

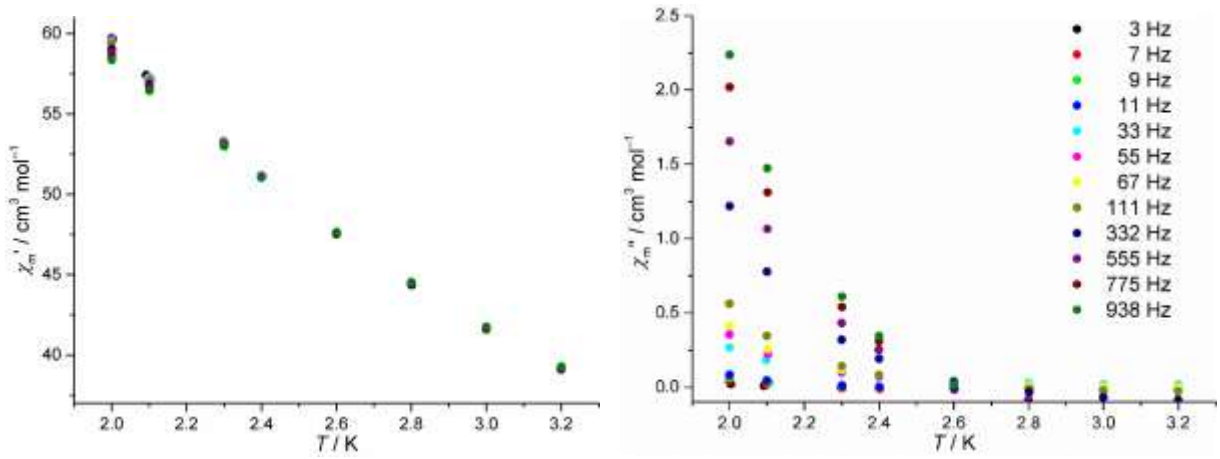

Figure S43. Temperature dependence of in-phase χ'_m and out-of-phase magnetic susceptibility χ''_m of **6** in absence of a static field *B*.